การเหนี่ยวนำการแสดงออกของ S100A7 ของเนื้อเยื่อโพรงประสาทฟันที่ได้รับแรง และผลต่อการสร้างเซลล์ทำลายกระดูก

นางสาวหทัยชนก เจริญพงศ์

วิทยานิพนธ์นี้เป็นส่วนหนึ่งของการศึกษาตามหลักสูตรปริญญาวิทยาศาสตรดุษฎีบัณฑิต
สาขาวิชาชีววิทยาช่องปาก
คณะทันตแพทยศาสตร์ จุฬาลงกรณ์มหาวิทยาลัย
ปีการศึกษา 2560

INDUCTION OF S100A7 EXPRESSION FROM MECHANICAL STRESS-INDUCED HUMAN DENTAL PULP CELLS AND ITS EFFECT ON OSTEOCLASTOGENESIS

Miss Hataichanok Charoenpong

A Dissertation Submitted in Partial Fulfillment of the Requirements
for the Degree of Doctor of Philosophy Program in Oral Biology
Faculty of Dentistry
Chulalongkorn University
Academic Year 2017

Thesis Title	INDUCTION OF S100A7 EXPRESSION FROM MECHANICAL STRESS-INDUCED HUMAN DENTAL PULP CELLS AND ITS EFFECT ON OSTEOCLASTOGENESIS
By	Miss Hataichanok Charoenpong
Field of Study	Oral Biology
Thesis Advisor	Assistant Professor Patcharee Ritprajak, Ph.D.

Accepted by the Faculty of Dentistry, Chulalongkorn University in Partial Fulfillment of the Requirements for the Doctoral Degree

.....Dean of the Faculty of Dentistry
(Assistant Professor Suchit Poolthong)

THESIS COMMITTEE

.....Chairman
(Professor Prasit Pavasant, Ph.D.)

.....Thesis Advisor
(Assistant Professor Patcharee Ritprajak, Ph.D.)

.....Examiner
(Associate Professor Thanaphum Osathanoon, Ph.D.)

.....Examiner
(Associate Professor Neeracha Sanchavanakit, Ph.D.)

.....External Examiner
(Assistant Professor Weerachai Singhatanadgit, Ph.D.)

หทัยชนก เจริญพงศ์ : การเหนี่ยวนำการแสดงออกของ S100A7 ของเนื้อเยื่อโพรงประสาทฟันที่ได้รับแรง และผลต่อการสร้างเซลล์ทำลายกระดูก (INDUCTION OF S100A7 EXPRESSION FROM MECHANICAL STRESS-INDUCED HUMAN DENTAL PULP CELLS AND ITS EFFECT ON OSTEOCLASTOGENESIS) อ.ที่ปรึกษาวิทยานิพนธ์หลัก: ผศ. ทญ. ดร.พัชรี ฤทธิ์ประจักษ์, หน้า.

การละลายของรากฟันโดยเซลล์ทำลายกระดูก สามารถพบได้หลังมีแรงกระทำต่อฟันและเนื้อเยื่อโพรงประสาทฟัน S100A7 มีบทบาทเกี่ยวข้องกับการอักเสบ อีกทั้งยังมีหลักฐานพบว่าอาจเกี่ยวข้องกับการทำลายกระดูก อย่างไรก็ตาม ยังไม่มีเคยมีการรายงานถึงบทบาทของ S100A7 ในเนื้อเยื่อโพรงประสาทฟัน การวิจัยนี้จึงทำขึ้นโดยมีวัตถุประสงค์เพื่อศึกษาผลของแรงกระทำต่อการแสดงออกของ S100A7 ในเซลล์เนื้อเยื่อโพรงประสาทฟัน และเพื่อศึกษาผลของโปรตีน S100A7 ต่อการสร้างเซลล์ทำลายกระดูก การศึกษานี้ได้ให้แรงกระทำต่อเซลล์เนื้อเยื่อโพรงประสาทฟันของมนุษย์ จากนั้นความมีชีวิตของเซลล์ได้ถูกทดสอบด้วยวิธีการของ MTT ระดับของ mRNA และความเข้มข้นของโปรตีนได้ทำการทดสอบด้วยวิธีการ Real-time PCR และ ELISA ตามลำดับ ในส่วนต่อมา เซลล์โมโนไซต์ปฐมภูมิของมนุษย์ได้ถูกนำมากระตุ้นให้พัฒนาไปเป็นเซลล์ทำลายกระดูก การสร้างและการทำงานของเซลล์สลายกระดูกถูกทดสอบด้วยการย้อมสีสำหรับ TRAP และการทดสอบการเกิดหลุมบนเนื้อเยื่อแข็ง ผลการทดลองพบว่าแรงกดไม่มีผลต่อความมีชีวิตของเซลล์เนื้อเยื่อโพรงประสาทฟัน ขณะที่แรงกดส่งผลให้มีการเพิ่มขึ้นของ mRNA ของสารอักเสบ *IL1B IL6 และ VEGF การแสดงออกของ* mRNA และระดับของโปรตีนของ S100A7 เพิ่มขึ้นอย่างมีนัยสำคัญหลังเซลล์ได้รับแรงกด อีกทั้งยังพบระดับของ mRNA ของ S100A7 เพิ่มขึ้น ในเนื้อเยื่อโพรงประสาทฟันของฟันที่ได้รับแรงในทางคลินิก เมื่อเทียบกับในฟันที่ไม่ได้รับแรง โปรตีน S100A7 มีผลส่งเสริมการสร้างเซลล์ทำลายกระดูกที่กระตุ้นด้วย RANKL และ M-CSF ทั้งยังพบว่า S100A7 เพิ่มการทำลายเนื้อเยื่อแข็งจากการทำงานของเซลล์ทำลายกระดูกอย่างมีนัยสำคัญอีกด้วย การแสดงออกของ mRNA ของ RAGE พบว่าเพิ่มขึ้นอย่างมีนัยสำคัญในระหว่างการสร้างเซลล์ทำลายกระดูกที่ถูกส่งเสริมด้วย S100A7 เทียบกับการไม่มี S100A7 การศึกษานี้สรุปได้ว่า แรงกระทำต่อเนื้อเยื่อโพรงประสาทฟันกระตุ้นการสร้าง S100A7 โดยโปรตีน S100A7 นี้อาจมีบทบาทเกี่ยวข้องกับการเกิดการละลายของรากฟัน โดยการส่งเสริมการสร้างและการทำงานของเซลล์ทำลายกระดูกที่ถูกกระตุ้นด้วย RANKL and M-CSF

สาขาวิชา ชีววิทยาช่องปาก ลายมือชื่อนิสิต .....

ปีการศึกษา 2560 ลายมือชื่อ อ.ที่ปรึกษาหลัก .....

5576058932 : MAJOR ORAL BIOLOGY
KEYWORDS: HUMAN DENTAL PULP CELLS / S100A7 / MECHANICAL STRESS / OSTEOCLAST

HATAICHANOK CHAROENPONG: INDUCTION OF S100A7 EXPRESSION FROM MECHANICAL STRESS-INDUCED HUMAN DENTAL PULP CELLS AND ITS EFFECT ON OSTEOCLASTOGENESIS. ADVISOR: ASST. PROF. PATCHAREE RITPRAJAK, Ph.D., pp.

Mechanical injuries of dental pulp tissues could lead to root resorption by osteoclast/odontoclast. S100A7 has been demonstrated to involve in inflammatory processes and potentially involved in bone destruction. However, the roles of S100A7 in dental pulp have not been reported. Therefore, this this study aimed to investigate the effect of mechanical stress on S100A7 expression in human dental pulp cells (hDPCs) and to investigate the effect of S100A7 protein on osteoclast differentiation. HDPCs were stimulated with *in vitro* compressive loading. Cell viability was determined using MTT assay. Real-time PCR (qPCR) and ELISA were utilized to determine the mRNA and protein levels, respectively. Further, osteoclast differentiation assay was performed using primary human monocytes. The differentiation and function of osteoclasts were examined using TRAP staining and resorption pit assay respectively. This study found that compressive mechanical stress did not affect viability of hDPCs while significantly stimulating expression of inflammatory cytokines *IL1B*, *IL6* and *VEGF* mRNA expression. S100A7 expression in both mRNA and protein levels was significantly increased following mechanical force application of hDPCs. Further, dental pulp tissues from the *in vivo* mechanical stress treated teeth exhibited higher *S100A7* mRNA levels compared with those of the control teeth. S100A7 promoted osteoclast differentiation from primary human monocytes in RANKL- and M-CSF dependent manner. In addition, S100A7 significantly enhanced resorptive pit formation *in vitro*. *RAGE* mRNA expression was significantly increased during S100A7-enhanced osteoclast differentiation. In conclusion, mechanical stress induced S100A7 expression in dental pulp and this protein may participate in root resorption via the enhancement of RANKL- and M-CSF- mediated osteoclast differentiation and function.

Field of Study: Oral Biology Student's Signature .....

Academic Year: 2017 Advisor's Signature .....

ACKNOWLEDGEMENTS

First, I would like to express my gratitude to my thesis advisor, Assistant Professor Dr.Patcharee Ritprajak, for her support and encouragement throughout my PhD work. I am also grateful to all my thesis committees in which their advice help improving my work.

I would like to express my sincere gratitude also to the head and the staffs in immunology laboratory, Faculty of Dentistry, Chulalongkorn University, for providing the protocol and supporting the instruments for the experiment.

I thank my fellow labmates. I appreciate their support in many aspects of my work. Lastly, I would like to express my gratitude to all the subjects participating in this study.

CONTENTS

Page

Page

List of Figures

List of Tables

Chapter 1

Introduction

Rationale and background

Root resorption is one of the conditions that can lead to loss of tooth. Root resorption either external or internal results from an action of osteoclast or odontoclast cells [1-4]. Root resorption can be physiologic when occurs during shedding of primary teeth. However, in many situations, it occurs as an unwanted effect [3, 5].

Various mechanical injuries such as dental trauma, chronic parafunctional force and uncontrolled orthodontic force can lead to root resorption [6, 7]. These mechanical injuries can trigger inflammation of dental pulp and endodontic treatment can decrease the prevalence, severity or stop the progression of root resorption [8-10]. In addition, studies also found the decrease in root resorption following orthodontic treatment in endodontically-treated teeth compared to untreated teeth [11-13]. These evidences support that root resorption can be trigger by the factors presented in dental pulp after mechanical stimuli.

Besides from external mechanical injuries, dental pulp cells may also encounter mechanical stress from the increase in intrapupal pressure during pulpal inflammation. Since pulp tissue is surrounded by mineralized tissue therefore it cannot expand. When there is the inflammation, the increase in intrapulpal pressure is observed [14]. Heyeraas and Berggreen 1999 [15] found an approximately 3-time increase in intrapulpal pressure in inflamed dental pulp compared to normal pulp.

S100A7 (psoriasin) is a low-molecular weight calcium binding protein first detected in keratinocytes of patients with psoriasis, an autoimmune-mediated chronic inflammatory disease [16] and was also reported to be upregulated in other skin inflammatory disease [17]. S100A7 can be induced by inflammatory cytokines such as interleukin (IL) 6 and oncostatin-M [18-21]. It can also stimulate the production of the production of various pro-inflammatory cytokines and chemokines such as IL-1α, IL-1β, IL-6, IL-8, Tumor necrosis factor (TNF) α and CXCL1 [22, 23]. In addition, S100A7 itself can be a chemotactic factor for leukocytes [23, 24] and promoting

angiogenesis by inducing vascular endothelial growth factor (VEGF). Thus, these indicate the role of S100A7 in tissue inflammation.

S100A7 may also play a role in osteoclast differentiation. Paruchuri *et al* [25] found that S100A7 down-regulated breast cancer cells demonstrated less bone destruction comparing to control cancer cells normally expressing S100A7. Furthermore, co-culture of S100A7 down-regulated breast cancer cells with mice bone marrow-derived osteoclast precursors also reduced the number of tartrate-resistance acid phosphatase (TRAP) positive cells.

Although there is the evidence that pulpal inflammation stimulated by mechanical injuries can lead to root resorption, the underlying mechanisms are still unclear. Since S100A7 involves in inflammatory reaction and was implicated in osteoclastogenesis, this study hypothesized that S100A7 was upregulated in human dental pulp following mechanical stress stimulation and S100A7 has the direct effect on differentiation of human osteoclasts.

Research question

Do human dental pulp cells (hDPCs) receiving mechanical stress induce S100A7 expression that can stimulate osteoclastogenesis?

Objectives of the study

1. To investigate the expression of S100A7 from mechanical stress-induced hDPCs
2. To determine the effect of S100A7 on differentiation of human osteoclast precursors into functionally active osteoclast.

Study hypotheses

1. **$H_0$1**: The mean fold change in *S100A7* mRNA expression in hDPCs receiving mechanical stress *in vitro* is not different from that of control cells not receiving mechanical stress

   H_a1: The mean fold change in *S100A7* mRNA expression in hDPCs receiving mechanical stress *in vitro* is different from that of control cells not receiving mechanical stress

2. **$H_0$2**: The mean level of *S100A7* mRNA in dental pulp tissue of teeth receiving mechanical stress *in vivo* is not different from that of control not receiving mechanical stress

   H_a2: The mean level of *S100A7* mRNA in dental pulp tissue of teeth receiving mechanical stress *in vivo* is different from that of control cells not receiving mechanical stress
3. **$H_0$3**: The mean concentration of S100A7 protein released from hDPC receiving mechanical force is not different from that of control cells

   H_a3: The mean concentration of S100A7 protein released from hDPC receiving mechanical force is different from that of control cells
4. **$H_0$4**: The mean fold changes in the number of osteoclasts are not different between osteoclast precursors differentiate with or without supplementation of S100A7.

   H_a4: The mean fold changes in the number of osteoclasts are different between osteoclast precursors differentiate with or without supplementation of S100A7.

5. **$H_0$5**: The mean fold changes in area of resorption are not different between osteoclast precursors differentiate with or without supplementation of S100A7.

   H_a5: The mean fold changes in area of resorption are different between osteoclast precursors differentiate with or without supplementation of S100A7.

Conceptual framework

Conceptual framework is illustrated in Figure 1

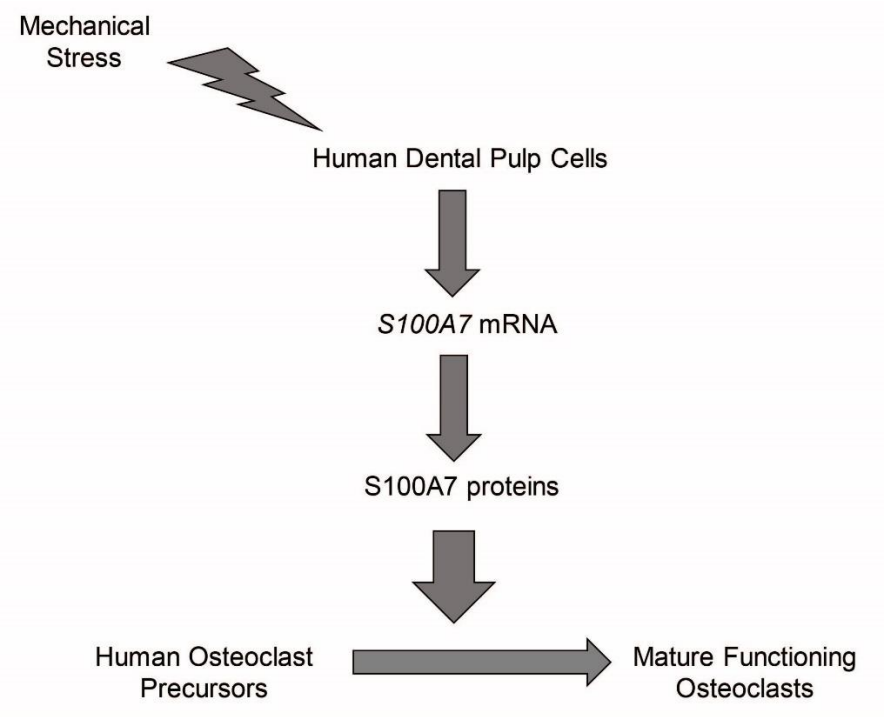

Figure 1 Conceptual framework of the study

Chapter 2

Review literatures

Dental pulp cell and its response to mechanical force

The main cell types found in dental pulp are odontoblasts, pulpal fibroblast, spindle shaped undifferentiated cells [26]. Occasionally, macrophage, dendritic cells and mast cell are also found [14]. Odontoblasts are the dentin producing cells locating periphery in a layer adjacent to dentin-pulp junction [27, 28]. Fibroblast and undifferentiated cells are morphologically similar in that they are stellated-like containing large nucleus with little cytoplasm (Figure 2). These undifferentiated cells have ability to form dentin-like complex [29] and also be able to differentiate into adipocyte and neural-like cells [30].

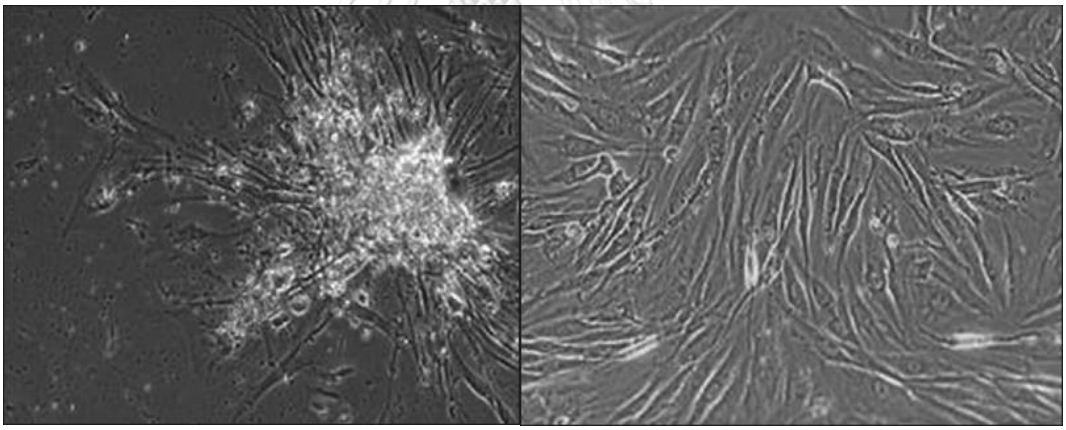

Figure 2 Morphology of mesenchymal cells from dental pulp from explant (left) to confluent (right) (picture from Shekar and Ranganathan [31])

In response to mechanical stress, various cell types produce inflammatory cytokines such as interleukin (IL)-1β, IL-6, IL-8 and tumor necrosis factor α (TNF-α) [32, 33]. Dental pulp cells also release inflammatory cytokines in response to mechanical compression force. Satrawaha *et al* [34] performed an *in vitro* study using a plastic cylinder containing metal coins placing on hDPCs cell layer to apply mechanical force onto the cells. This study found that mechanical stress ranging from 0.7 to 1.4 g/cm^2 can upregulate the *IL6* mRNA expression in hDPCs. Upregulation of

IL6 mRNA was found from 2 hours to 24 hours after force application while significantly increase in IL-6 protein release was found from 4 hours onward. This pressure induced IL-6 expression was mediated by P2Y6 receptor. This study also reported that application of 1.4 g/cm^2 of force for 16 hours onto hDPCs did not affect cell viability and cell morphology. Increase in *IL6* mRNA and protein expression was also observed in stem cells from human exfoliated deciduous teeth (SHED) exposed to 2.5 g/cm^2 of mechanical force for 2 hours without affecting cell viability [35].

Blesta *et al* [36] studied in Wistar rat using immunostaining after applying orthodontic force and found that there was a minor different in expression of IL-1α in pulp of control and force applied teeth of the rats. However, there was an increase in cells positively stained for TNF-α especially in the pulp body at day 3 after force application indicating that there was an aseptic pulpitis occurred as a result of mechanical force.

Lee *et al* [37] reported that mechanical strain can induce hDPCs to produce inflammatory cytokines such as IL-β, TNF-α, and IL-6. In addition to inflammatory cytokines, this study also found the upregulation of some antioxidant genes which may act as a defense mechanism of hDPCs to mechanical stress.

It was also reported that mechanical stress can enhance odontoblastic differentiation of dental pulp cells. Yu *et al* [38] use a hydrostatic pressure device to apply the force 1.5-3 MPa to dental pulp stem cells (DPSCs). The force apply was intermittent with the frequency of 0.5 Hz or 5 cycle per 10 seconds. It was found that DPSCs exhibited morphological change after application of hydrostatic force in dose and time dependent pattern. There was also an insignificant decrease in cell viability after 12 hours of force application. However, cell viability was recovered after elimination of the force. Moreover, pressure was found to enhance the odontoblastic differentiation in these DPSCs compared to the control cells without application of pressure. The mechanical stressed-induced osteoblastic differentiation of DPSCs was also reported in the study of Lee *et al* [39] that introduce the cyclic tensile strain to the cells. This effect was found to be mediated by heme oxygenase-1 (HO-1) pathway.

In response to orthodontic force, hDPCs can also release calcitonin gene-related peptide (CPRG). Caviedes-Bucheli*et al* [40] studied CPRG expression in human dental pulp collected after the teeth have been subjected to orthodontic force.

CPRG is the neuropeptide released from nerve fibers including those in dental pulp and can trigger vasodilation, plasma extravasation and recruitment of inflammatory cells. This study found that there was a significant different in CPRG protein level in dental pulp of teeth subjected to 24-hour of heavy force, medium force and no force group with the highest CPRG level was found in heavy force followed by medium force and no force control group respectively.

S100 protein family

S100 proteins are the low-molecular-weight proteins. They are usually 10-12 kDa [41]. S100 protein family is the largest family among EF-hand protein superfamily [42]. The proteins in S100 protein family contains the C-terminal canonical calcium-binding EF-hand motif and an N-terminal non-canonical EF-hand motif (Figure 3). At present, more than 20 members have been identified and most of their genes are located on chromosome 1q21 [41, 43, 44]. The list of S100 proteins that have been discovered is shown in Table 1

S100 proteins usually present in dimeric form, either homodimeric or heterodimeric (Figure 3) and are found in various tissues [44, 45]. Upon binding to calcium, most S100 proteins undergo a conformational change, allowing them to interact with the different targets producing a wide range of functions [43-45].

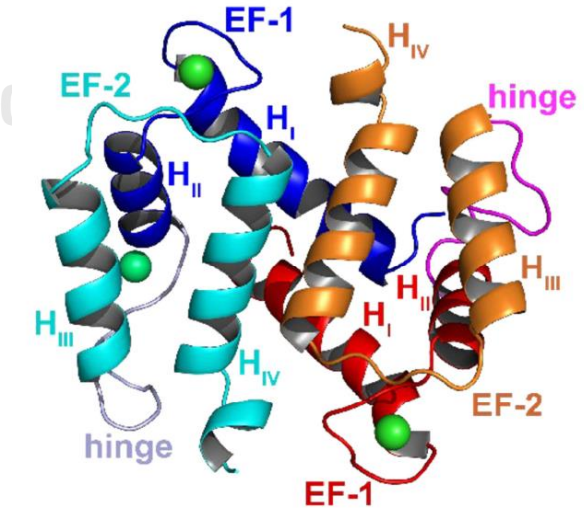

Figure 3 Dimeric structure of S100 protein (Picture from Srikrishna and Freeze [44])

Table 1 The approved gene name of known S100 proteins from Salama et al [46]

Approved gene symbol (gene name)	Other names and obsolete names
S100A1	S100A, S100
S100A2	S100L.CaN19
S100A3	S100E
S100A4 (metastasin, calvasculin)	MTS1, CAPL, p9KA, pEL98, 18A2, 42A
S100A5	S100D
S100A6 (calcyclin)	CACY, 2A9, CABP, 5B10, PRA
S100A7 (psoriasin)	PSOR1
S100A7L2 (S100A7-like 2)	S100a7b
S100A7L3 (S100A7-like 3)	S100A7d
S100A7L4 (S100A7-like 4)	S100A7e
S100A8 (calgranulin A)	CAGA, MRP8, P8, CGLA, MIF, NIF, L1Ag, MAC387, 60B8AG, CFAG
S100A9 ((calgranulin B)	CAGB, MRP14, P14, CGLB, MIF, NIF, L1Ag, MAC387, 60BAG, CFAG
S100A10 (annexin II ligand; calpactin I, light polypeptide)	ANX2LG, CAL1L, CLP11, ANX2L, p11, p10, 42C,GP11
S100A11 (calgazzarin)	S100C, LN70
S100A11P (S100A11 pseudogene)	S100A14
S100A12 (calgranulin C)	CAAF1, CGRP, MRP6, p6, ENRAGE
S100A13	
S100A14	BCMP84, S100A15
S100A15	S100A7L1, S100A7a
S100A16	S100F, DT1P1A7, MGC17528
S100B	S100β
S100P	
CALB3 (calbindin 3)	Calbindin D9k, CaBP9k, CABP1

The roles of S100 proteins extensively study are the roles in cancer which include regulation of cellular differentiation, stem properties, tumor environment, cell invasion and migration, apoptosis, cell growth and cell cycle [45]. The roles of each S100 in cancer are summarized in Figure 4

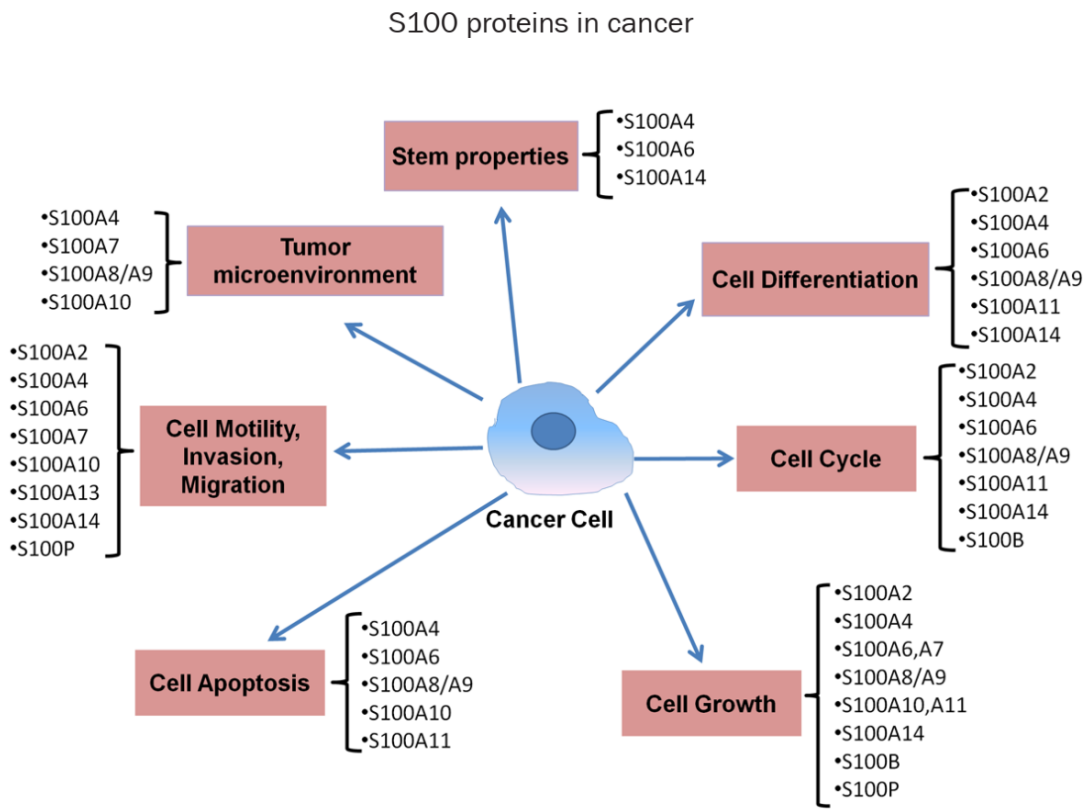

Figure 4 The reported function of S100 in cancer biology (Picture from Chen, Xu and Liu 2014 [45])

S100 proteins can function intracellularly as well as extra cellularly. Intracellular functions of S100 proteins include the regulation of cell proliferation, differentiation, apoptosis, Ca^{2+} homeostasis, inflammation, cell growth, cell cycle and cell migration/invasion [43, 45]. S100 proteins that can have intracellular functions include S100A1, S100A2, S100A4, S100A6, S100A7, S100A11 and S100B [43, 46]. Some intracellular functions of each S100 are summarized in Figure 5

Extracellulary, S100 proteins can function as cytokines that can regulate cellular activity upon binding to various types of cell surface receptors including the receptor for advanced glycation end products (RAGE) and toll-like receptors (TLRs), IL-10

receptor (IL-10R), CD166 antigen (also known as ALCAM), fibroblast growth factor receptor 1 (FGFR1) and extracellular matrix metalloproteinase inducer (EMMPRIN or basigin) [45, 47].Therefore, extracellular S100 proteins can interact with various cell types including monocytes, macrophages, lymphocytes, neutrophils, mast cells, epithelial cells, neurons, Schwann cells and vascular smooth muscle cells [43]. The S100 proteins that have been found extracellularly include S100B, S100A4, S100A7, S100A8, S100A9, S100A12, and S100A13 [45, 47]. The reported extracellular functions of S100 proteins include regulation of cell migration, tumor invasion, tissue development and repair and participating in innate and adaptive immune responses [43, 48]. Figure 5 showed some of the reported extracellular functions of each S100.

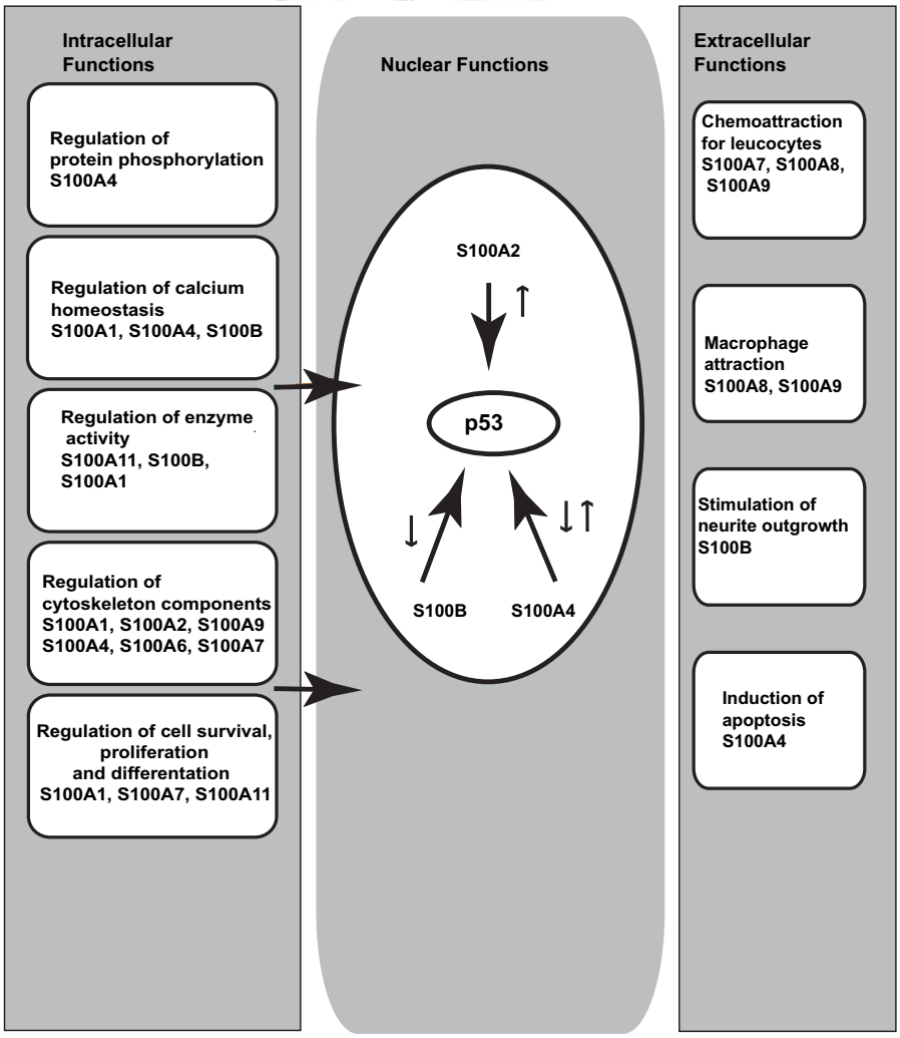

Figure 5 The reported intra- and extracellular function of S100 (Picture from Salama et al [46])

S100A7

S100A7 (psoriasin) protein has the molecular weight of 11.4 kDa [16]. Its gene is located within the epidermal differentiation complex on chromosome 1q21 and usually contains 3 exons and 2 introns with the genomic organization similar to other S100 proteins [49]. The first exon encodes the 5' untranslated region while exon 2 and exon 3 contain the all the coding sequences. The N-terminal and C-terminal EF-hand binding motif of S100A7 are encoded from exon 2 and exon 3 respectively (Figure 6) [49, 50]. S100A7 proteins usually form a homodimeric structure with one calcium ion bound by EF hand motif in each subunit and two zinc ions located between two subunits (Figure 7) [51]. However, S100A7 has low affinity of binding to calcium and zinc and unlike most of S100 proteins, S100A7 does not undergo a large conformation changes upon binding to calcium [51].

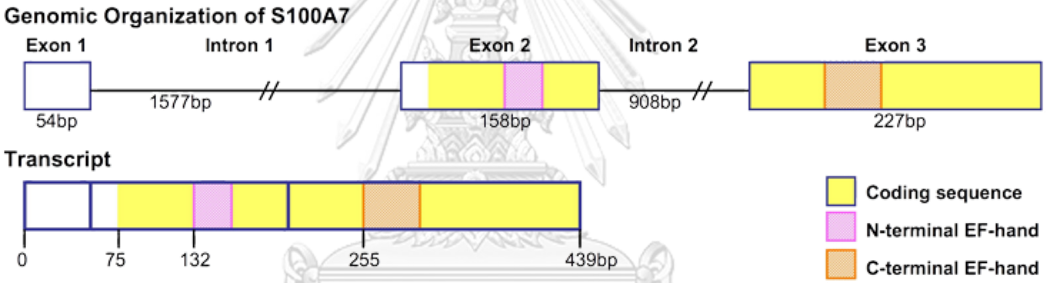

Figure 6 The genomic organization of S100A7 includes 3 exons and 2 introns. Exons 2 and 3 containing the protein encoding sequence. (Picture from http://atlasgeneticsoncology.org /Genes/S100A7ID42194ch1q21.html)

Expression and localization of S100A7

S100A7 was first detected in keratinocytes of patients with psoriasis [16] and was also reported to found highly expressed in atopic dermatitis [17]. In normal condition, expression of S100A7 is restricted in epithelial part of tissues such as in keratinocytes, breast epithelial cells and bladder epitheliums [49, 52]. S100A7 can be found as nuclear, cytoplasmic proteins and secreted proteins. Upregulation of cytoplasmic as well as secreted S100A7 was observed when stimulated with calcium and retinoic acid in abnormal pathways of differentiation of keratinocytes [49, 52].

Ruse, Broome and Eckert [53] also found that S100A7 was in cytoplasm of untreated keratinocytes while localized in cell periphery when stimulated with calcium.

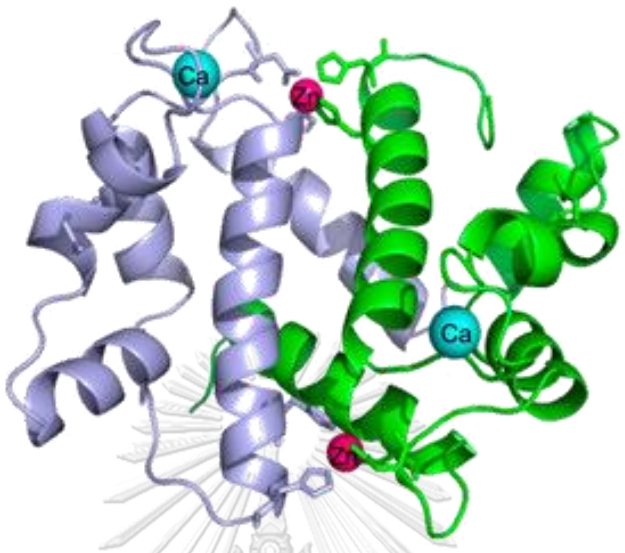

Figure 7 Dimeric structure of S100A7 with zinc and calcium bound. (picture from http://atlasgeneticsoncology.org/Genes/S100A7ID42194ch1q21.html)

S100A7 was also found in nucleus and cytoplasm of breast cancer cells and also found secreted by these cells [54, 55]. Although S100A7 is expressed in normal epithelium, the level is relatively low. High level of S100A7 was observed in breast carcinoma in situ and in subset of invasive breast cancers [47, 52]. In addition, S100A7 expression level are associated with unfavourable features of breast cancer [52]. Dramatically increase in S100A7 expression was also observed in mammary epithelial cells stressed cells induced by growth factor deprivation, cell confluency and loss of attachment to extracellular matrix [55].

Biological roles of S100A7

S100A7 has both extracellular and intracellular functions. Its reported functions include antimicrobial function, lipid transport, regulation inflammatory cytokine production, angiogenesis, leukocyte chemotaxis, tumor progression, promoting viability and suppression differentiation of cancer cells [18]. The major roles of S100A7 are in cancer and tissue inflammation.

Roles of S100A7 in cancer

S100A7 has a distinct role in breast cancer cells. It has different effect depending on estrogen receptor (ER) status of these cells. S100A7 tend to suppression tumor with estrogen receptor-α (ERα)-positive cells but promotes tumors growth and metastasis in ERα-negative cells. In ERα-positive breast cancer cells, S100A7 was reported to inhibit tumor growth by suppressing the β-catenin/T cell factor 4 (TCF4) pathway [56].

In ERα-negative breast cancer cells, on the other hand, S100A7 overexpression is associated with more aggressive and worse prognosis features of the cancer [57]. S100A7 binding to c-Jun activation domain-binding protein 1 (Jab1) and activation of nuclear factor-kB (NF-κB) and phospho-Akt can promotes growth and survival of these ERα-negative breast cancer cells [43, 45, 57, 58]. In addition, S100A7 was also reported to enhance cell survival and invasion in ERα-negative breast cancer cells through upregulation of epidermal growth factor receptor (EGFR) signaling [25]. It was found that in S100A7 down-regulated breast cancer cells, there was a reduction in phosphorylation of EGFR and reduction of Scr phosphorylation when stimulated with EGF [25].

The secreted S100A7 from cancer cells can also bind to RAGE on macrophages and endothelial cells and mediate the recruitment of tumor-associated macrophages and promoting angiogenesis in tumor [23, 47]. S100A7 may also induce angiogenesis in tumors via regulating expression of vascular endothelial growth factor (VEGF) [23, 59]. S100A7 down-regulated breast cancer cell showed significant down-regulation of S100A7 [59] and expression of S100A7 in primary breast tumor was found associated with increase in angiogenesis that may result in an increase metastasis of tumor [59]. Increase bone invasion of breast cancer cell was also observed in S100A7 down-regulated cells by regulation of osteoclast which as described in the following section.

S100A7 interaction with RAGE was also reported to enhance invasion and migration of osteosarcoma cells [45, 60]. S100A7 is also involved in matrix remodeling in tumor environment. Increases invasion of prostate cancer cells by S100A7 was reported through regulation of MMP [45]. The role of extracellular S100A7 in tumor progression was illustrated in Figure 8

However, although S100A7 tends to promote tumor growth and invasion, some contrary has been reported. Krop *et al* [59] found that down regulation of S100A7 in breast cancer cells was associated with increase in MMP13. In this study, S100A7 was reported to have a role in decreasing local invasion but promote metastasis by increase VEGF. S100A7 was also reported to inhibit cell growth in oral squamous cell carcinoma by regulating β-catenin degradation [45, 47].

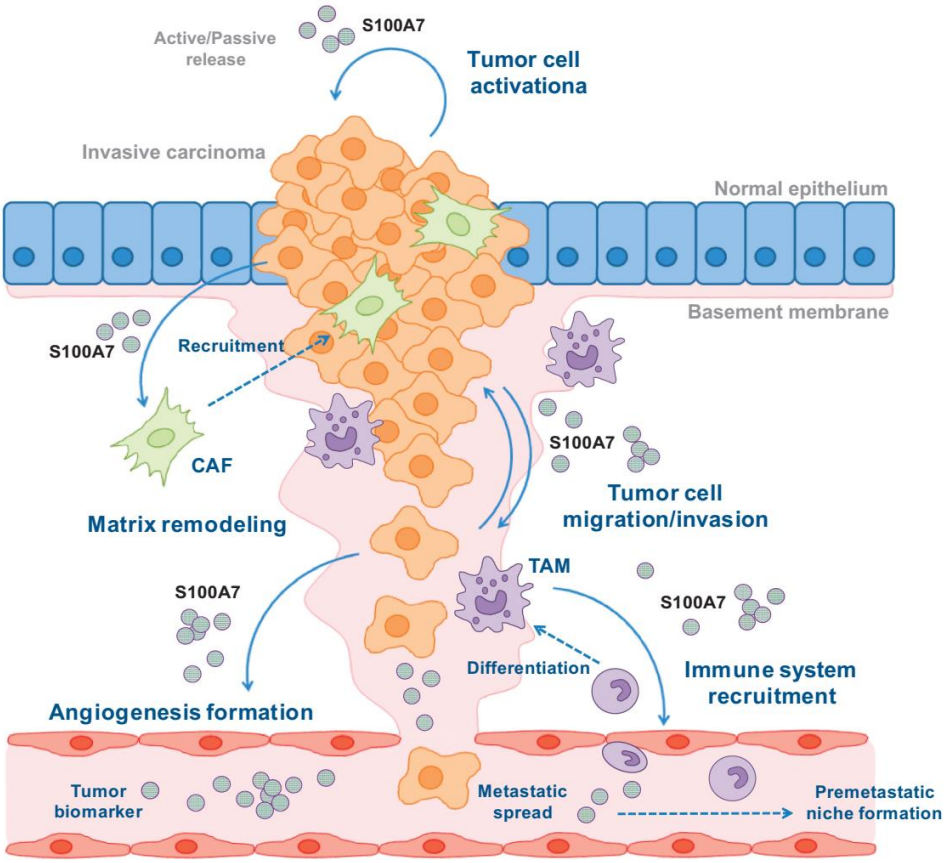

Figure 8 The roles of S100A7 in tumor progression include recruitment of immune cells, stimulate the factors involved in matrix remodelling, migration and invasion of tumor and angiogenesis; CAF=cancer associated fibroblast, TAM=tumor associated macrophage. (Picture from Padilla et al [61])

Roles of S100A7 in inflammation

S100A7 expression in skin inflammatory diseases

S100A7 was associated with skin inflammatory diseases as it was detected in high level in keratinocytes of patients with psoriasis, an autoimmune-mediated chronic

inflammatory disease [16]. More recently, S100A7 was also reported to found in atropic dermatitis [17]. Up to 1500-fold increase in the level of S100A7 was observed by ELISA in skin with atropic dermatitis compared to control healthy skin [17].

Induction of S100A7 by inflammatory cytokines

Studies have found that S100A7 can be induced by several inflammatory cytokines (Table 2). TNF-α, IL-17 and IL-22 were reported to induce S100A7 in keratinocytes [17, 20, 62] with the stronger induction of S100A7 was found when stimulated with IL-22 in combination with IL-17, IL-17A or IL-17F [17, 20]. The induction of S100A7 by IL-17 was reported to act through ERK (extracellular signal-regulated kinase)-Egr1 (early growth response 1) pathway [18]. In addition, Gazel *et al* [19] found that S100A7 can be induced by oncostatin-M in human epidermal cell skin equivalents (reconstituted human epidermis) in both mRNA and protein level. West and Watson [21] also reported that S100A7 was induced by oncostatin-M and IL-6 in MCF7, T47D and MDA-MB-468 breast cancer cell lines in dose- and time-dependent manner. The induction of S100A7 by these two cytokines was found to be regulated by STAT3, phosphatidylinositol 3 kinase (PI3K) and ERK1/2 signaling pathway [21]. IL-8 also have been reported to induce S100A7 [18].

Induction of inflammatory cytokines and chemokines by S100A7

S100A7 can trigger the production of various pro-inflammatory cytokines and chemokines (Table 2). Batycka-Baran et al [22] found that S100A7 can significantly induce IL-1β, IL-6, TNF-α and IL-8 in peripheral blood mononuclear cells (PBMC) in both transcriptional and protein levels. However, the Th2 cytokines, IL-17A, IL-4 and IL-5 were not found to be induced by S100A7 in this study.

Zheng et al [63] reported that S100A7 can trigger neutrophils to produce inflammatory cytokines and chemokines including IL-6, IL-8/CXCL8, TNF-α, macrophage inflammatory protein-1α (MIP-1α)/CCL3, MIP-1β/CCL4 and MIP-3β/CCL20 through activation of MAPK p38 and ERK. Nesser *et al* [23] found that overexpression of S100A7 in breast cancer cell lines can induce inflammatory cytokines and chemokines include CXCL1, CXCL8, IL-1α, IL-11 and CSF2. In

addition, S100A7 itself can be the chemotactic factor for granulocytes lymphocytes and monocytes/macrophages via interaction with RAGE receptor [23, 24].

Table 2 List of cytokines/chemokines that stimulate S100A7 expression and/or are induced by S100A7

Cytokine/Chemokine	Stimulator of S100A7	Induced by S100A7
TNF-α	✓	
IL-17	✓	
IL-22	✓	
Oncostatin M	✓	
IL-6	✓	✓
IL-8/CXCL8	✓	✓
IL-11		✓
IL-1α		✓
IL-1β		✓
MIP-1α/CCL3		✓
MIP-1β/CCL4		✓
MIP-3β/CCL20		✓
CXCL1		✓
CSF2		✓

Regulation of S100A7 expression

Beside from the inflammatory cytokines shown above, production of S100A7 may be induced by EGF, EGF-like growth factors, lipocalin-2, visfatin, P2X7 and EphA2 receptor activation [18, 25].

Evidences showed that EGFR may involves in S100A7 production. It was found expressed in correlation with expression of S100A7 in psoriasis and in ER-negative breast cancers [18, 64]. Blocking of EGFR can suppress oncostatin M induced S100A7 [21]. Studies in cancer cells also found that S100A7 expression was increased following stimulation with EGF [25]. For EGF-like growth, study indicated that it may stimulate

S100A7 in synergistic with IL-1 [18]. Lipocalin-2 is an antimicrobial protein and adipokine potentially increase mRNA expression of S100A7 in mouse skin. Lipocalin-2 may also have the autocrine effect to stimulate the production of S100A7 from keratinocytes [18]. Visfatin level was found increase in psoriatic sera compared to control. It was found that visfatin may act in synergistic with TNF to induce S100A7 expression [18]. Erythropoietin-producing hepatocellular A2 receptor (EphA2) was found increase in its expression in psoriasis. Increase in EphA2 was also reported to induce S100A7 overexpression in keratinocytes. P2X7 was found up-regulated in psoriasis and its activation resulted in an increase S100A7 expression [18].

In contrast, production of S100A7 may be suppressed by IL-4 and IL-37. Onderdijk *et al* [65] found the significant decrease S100A7 expression in normal skin after culturing in the presence of IL-4. Moreover, IL-4 was found to significantly inhibit IL-1b–induced S100A7 expression [65]. IL-37 overexpression in keratinocytes can suppress the expression of S100A7 [66]. These down-regulation of S100A7 was found coincide with down-regulation of CXCL8 and IL-6. Therefore, S100A7 suppression may be regulated directly by the effect of IL-37 or as a result of down-regulation of CXCL8 and IL-6 since these two cytokines was found to have the stimulatory effect on S100A7.

Osteoclast

Osteoclasts are large multinucleated cells differentiated from hematopoietic stem cells through the fusion of multiple mononuclear myeloid precursors [67-70]. When becoming mature osteoclasts, they are capable of resorbing bone. In order to resorb bone, osteoclasts adhere to bone surface and form the sealing zone isolating the resorption lacunae from surrounding area [71]. Osteoclasts then create low pH environment in resorption lacunae using ion transport along with the action of intracellular carbonic anhydrase 2 enzyme. This acidic environment can dissolve of inorganic component of bone while bone matrix is degraded by proteolytic enzyme such as cathepsin K and tartrate resistance acid phosphatase (TRAP) [68] (Figure 9).

Osteoclastogenesis is a multistep process regulated by various biological molecules that can be mainly divided mainly into those involving in main signaling

pathway from RANKL and M-CSF, co-stimulatory pathway, integrin pathway and others.

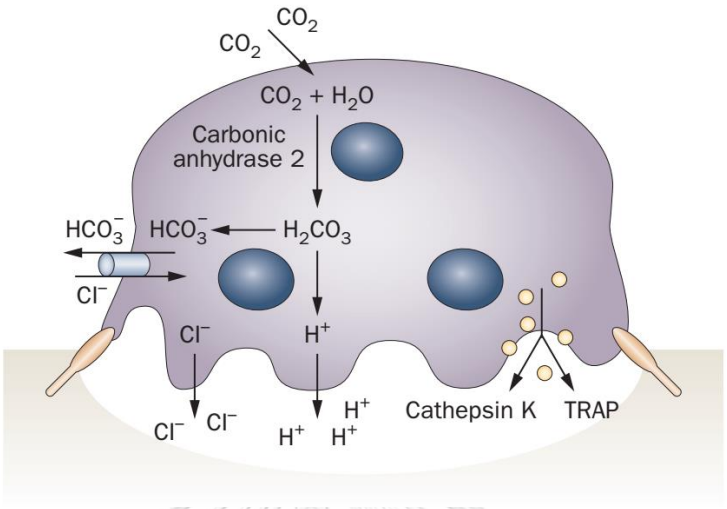

Figure 9 Diagram of mature osteoclast resorbing bone (Picture from Edward and Mundy [68])

Main signaling pathway in osteoclastogenesis

Two key cytokines important for differentiation and maturation of osteoclast are macrophage colony-stimulating factor (M-CSF) and receptor activator of NF-kB ligand (RANKL).

M-CSF interact with its receptor c-Fms on osteoclast precursors as well as mature osteoclasts [69]. Expression of c-Fms is controlled by PU.1 transcription factor. Binding of M-CSF to its receptor leads to activation of many signaling pathways including PI3k/AKT/mTOR, c-Jun N-terminal kinase (JNK), ERK and Src pathways leading to recruitment of transcription factors such as AP-1 [68, 72-74] (Figure 10).

With the stimulation of M-CSF, hematopoietic stem cells differentiate into macrophage colony-forming units (CFU-M), precursors of macrophages and osteoclasts cells [75]. M-CSF is essential in proliferation and survival of these precursors [73, 74]. In addition, M-CSF can stimulate expression of receptor activator of nuclear factor-kB (RANK) in monocyte–macrophage precursors therefore enhancing the response to RANKL in the following stage of differentiation [74].

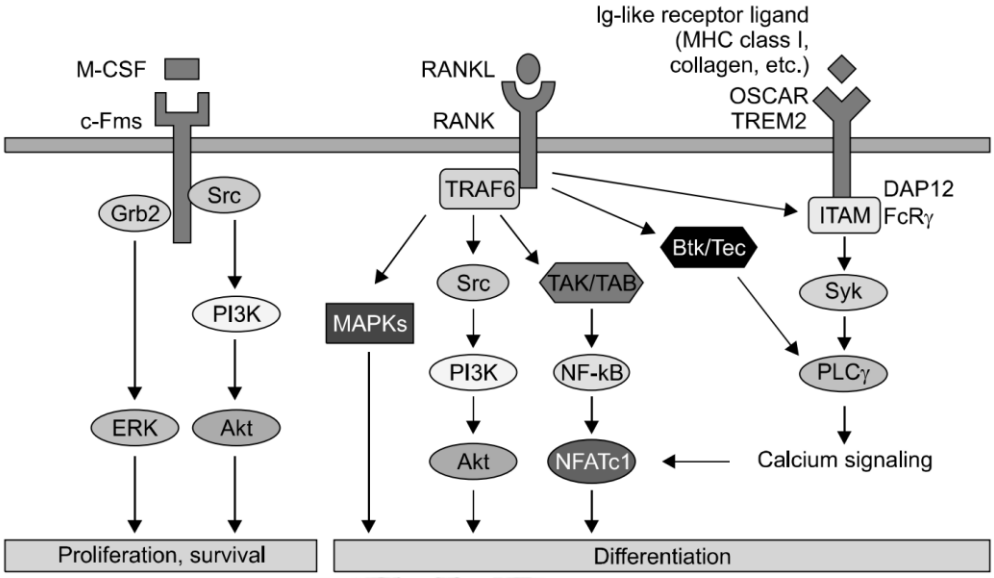

Figure 10 Main and co-stimulatory signaling pathways regulating osteoclast differentiation (picture from Kim and Kim 2016 [76])

Signaling pathway from RANK-RANKL interaction is well-established for osteoclast differentiation. Upon binding of RANKL to its receptor RANK, tumor necrosis factor receptor-associated factor (TRAF) 2 and TRAF5 are recruited to the receptor complex leading to subsequent recruitment of TRAF6. TRAF6 is the main adaptor molecule for RANK-RANKL mediated osteoclast differentiation and function [69, 74]. Recruitment of TRAF6 results in phosphorylation of the IkB protein and subject IkB to proteasomal degradation leading to releasing of active NFκB. The transcription factor most strongly induced by NFκB is NFATc1 which is considered as the master regulation of osteoclast [77]. The target genes of NFATc1 includes TRAP, cathepsin K and calcitonin receptor which are the genes important for osteoclast function [75, 78]. Signal from RANKL also induces the activation of mitogen-activated protein kinase (MAPK) (p38, JNK, ERK) as well as c-Src/PI3k/AKT pathway [69, 73] which contribute to activation NFATc1 as well as AP-1 family of transcription factors [68, 70, 79] (Figure 10).

Signal from RANKL is required for the later stage of osteoclast differentiation characterized by intracellular fusion and maturation into functioning osteoclast after earlier stimulation by m-CSF [75]. Osteoclast precursors expressing RANK, when stimulated by RANKL will exit cell cycle and fuse together to form multinucleated

osteoclasts [73]. RANKL is also important for the resorption activity of mature osteoclasts [69].

Co-stimulatory pathway through immunoreceptor tyrosine-based activation motif (ITAM)–associated receptors

Apart from the two main signaling pathways, m-CSF and RANKL, there are the co-stimulatory pathways that contribute in part to the differentiation of osteoclast although whether these pathways alone are capable to induce formation of osteoclast is still controversy.

The two well-known receptors that produce co-stimulatory signal for osteoclast differentiation are osteoclast-associated immunoglobulin-like receptor (OSCAR) and triggering receptor expressed on myeloid cells 2 (TREM-2) [78, 80]. Both of them associate with immunoreceptor tyrosine-based activation motif (ITAM) haboring adaptor. OSCAR associates with Fc receptor common γ subunit (FcRγ) and TREM-2 associates with DNAX-activating protein 12 (DAP12). Together with signal from RANKL, co-stimulatory signal from these ITAM harboring receptors activate Syk and phospholipase Cγ (PLCγ) [81], which then hydrolyses phosphatidylinositol-4,5-bisphosphate (PIP2) into inositol-1,4,5-trisphosphate (IP3) and diacylglycerol. IP3 stimulates the influx of Ca2+ from ER. Binding of calcium to calmodulin, in turn, activates Calcineurin, the calmodulin-dependent phosphatase which dephosphorylate NFATc1. Dephosphorylation of NFATc1 results in its activation and nuclear translocation [78] (Figure 10). Therefore, this ITAM-mediated signal provide co-stimulatory signals to maximize the activation of NFATc1 in RANKL-mediated osteoclastogenesis [78].

Integrin signaling pathway

Integrin signaling is important for osteoclast function. When function to resorb bone, osteoclasts require tight binding to the bone surface and formation of ruffled border. This process is induced by integrin αvβ3 [68, 82]. Mature osteoclasts express high levels of the integrin αvβ3 [71]. The ligands of αvβ3 integrin include bone matrix proteins, osteopontin, vitronectin and bone sialoprotein [71].

Stimulation of αvβ3 by its ligand results in phosphorylation and activation of c-Src which is associated with β3 subunit [82]. Activated c-Src phosphorylates Syk, which then recruits Slp76, an adaptor of Vav3 [82]. Vav3 can activate small GTPases of the Rho family in which the key effector molecules of αvβ3 integrin are Rac1 and Rac2 [82]. The resulting activation of αvβ3 integrin signaling leads to cytoskeleton organization that allow activation and function of osteoclasts [82] (Figure 11). Signaling from αvβ3 integrin also have a crosstalk with other signaling in osteoclast differentiation includes signal from M-CSF and RANKL [82-84].

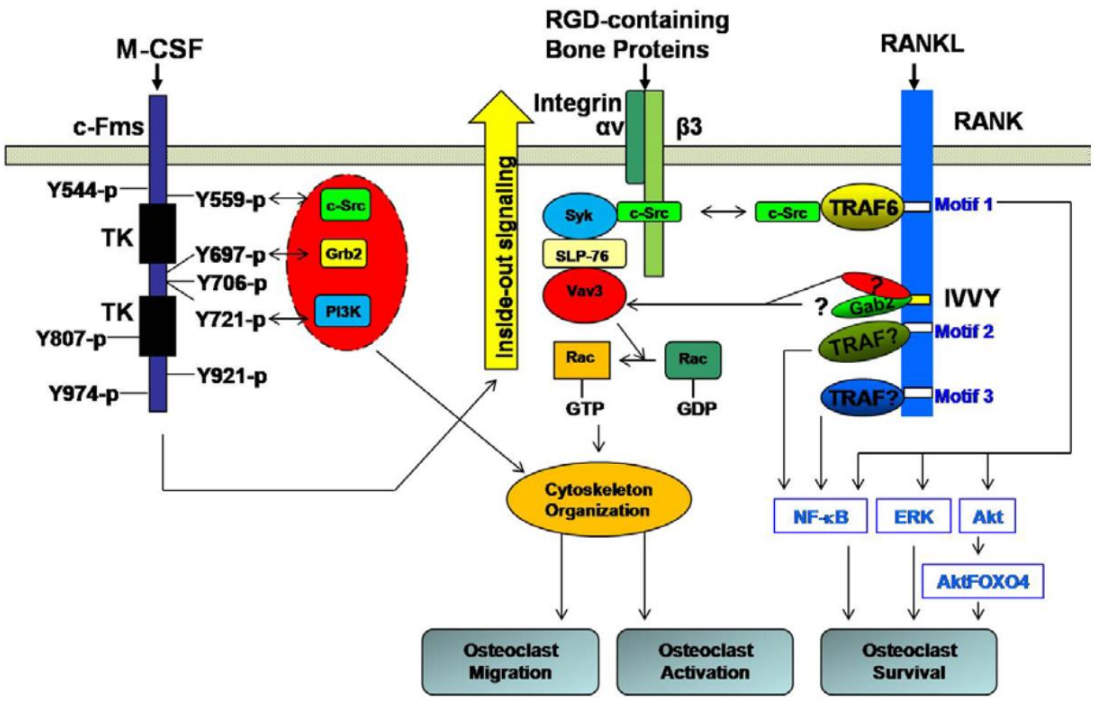

Figure 11 Integrin signalling pathway in osteoclast differentiation and function (Picture from Feng and Teitelbaum [82])

Other molecules affecting osteoclast differentiation

In addition to the molecules in main signaling pathway and co-stimulatory pathway from ITAM-associated receptors, there are some other biological molecules have been reported to stimulate osteoclast differentiation. Whether these non-canonical pathways of osteoclast activation are RANKL-independent or not is still controversy [85]. The roles of these molecules in physiologic bone resorption are still uncertain. However, it is likely that the non-canonical pathways of osteoclast differentiation may

have a role in pathological bone resorption [69]. The cytokines, growth factors, danger signal or hormones that involve in non-canonical pathway of osteoclast differentiation may be divide into those that can substitute or at least have the additional effect for RANKL or M-CSF on osteoclast differentiation [69, 73, 86].

The reported cytokines that possess the effect of M-CSF include VEGF, FLt-3 ligand, hepatocyte growth factor (HGF) and placental growth factor (PlGF) [73, 86]. The biological molecules possess RANKL effect include the factors that are TNF superfamily members such as TNFα, lymphotoxin exhibiting inducible expression and competing with herpes simplex virus glycoprotein D for herpesvirus entry mediator, a receptor expressed by T lymphocytes (LIGHT), a proliferation inducing ligand (APRIL) and B cell activating factor (BAFF) and those that are not TNF superfamily members such as IL-6, IL-11, IL-8, transforming growth factor β (TGF-β), nerve growth factor (NGF) and insulin-like growth factor-I (IGFI), interferon γ (IFN- γ) [69, 86, 87]. These factors can have direct effects on osteoclasts and some also have indirect effects by upregulate of RANKL expression in other cell types [87]. RANKL expression can also stimulated by factors such as IL-17, and oncostatin M, and hormones, such as 1,25-dihydroxy vitamin D3 (1,25$(OH)_2$D3), parathyroid hormone (PTH) [69, 73]. Therefore, these factors can also indirectly regulate osteoclast differentiation.

S100 proteins and osteoclasts

TLR and RAGE, the receptors for S100 proteins were found to express in osteoclast (Bar-Shavit 2008; Kosaka et al. 2014). The effect of TLR on osteoclast depends on the stage of differentiation. Activation of TLR in early osteoclast precursors inhibits its differentiation. However, TLR activation can promote differentiation and survival of mature osteoclasts [87, 88].

RAGE and its ligands can stimulate osteoclastic activity [89]. It was found that RAGE mRNA and protein expression is upregulated during osteoclast differentiation [89, 90]. RANKL has been shown to be able to stimulate expression of RAGE [84]. Bone marrow macrophages of RAGE mutant mice have the defect in differentiation and maturation into osteoclasts in response to RANKL [89]. RAGE-deficient mice exhibited the increase in bone mass and bone mineral density [89, 90].

S100 proteins can interact with RAGE and TLR, therefore may have a role in stimulation of osteoclastogenesis. S100 proteins is found to express in normal bone cells including osteoblast and chondrocytes as well as in pathological bone tissues such as osteosarcoma, ossifying fibromyoloid tumor, osteoid osteoma, chondrosarcoma, and bone cells in teratoma [89]. The S100 proteins that have been reported to be implicated in activation of osteoclast include S100A4, S100A7 and S100A8.

Recombinant S100A4 (1μg/ml) was found to significantly increase the number of $TRAP^+$ cells derived from mice bone marrow macrophage precursors [91]. However, the bone resorption was not investigated in this study. Erlandsson *et al* [92] demonstrated the bony characteristics of S100A4 deficient mice which include higher bone mass, increased trabecular number and thickness combined with larger periosteal circumference. These S100A4-deficient characteristics was also confirmed by S100A4-shRNA knock down of S100A4 in wild-type mice. These characteristics were contributed to the hyperactivity of osteoblasts and also the suppression of functional osteoclasts in S100A4 deficient mice. It was also found that S100A4 deficient osteoclasts exhibited poor multinucleation, morphological change, lower level of proteolytic enzymes, lower integrin level and impaired adhesion capacity.

S100A7 is also implicated in osteoclastogenic. Paruchuri *et al* [25] found that S100A7 down-regulated breast cancer cells demonstrated less bone invasion comparing to control cancer cells which normally express S100A7. Furthermore, when culture mice bone marrow-derived osteoclast precursor in transwell assay with S100A7 down-regulated breast cancer cells, there was a decrease in the number of TRAP positive cells when compared to co-culture with breast cancer cells transfected with control vectors or the positive control induced with RANKL. However, the ability of these $TRAP^+$ cells to resorb mineralized tissue was not investigated. This study also showed that the effect of S100A7 mediated osteoclast formation might be associated with IL-8 since S100A7 down-regulated cells showed the decrease in the production of IL-8, the cytokine that can stimulate osteoclastogenesis.

S100A8 and S100A9 were found abundantly expressed in osteoclast [93]. However, Grevers *et al* [94] found that the ability to differentiate into osteoclast from precursors cells derived from S100A8/A9 deficient mice was not affected compared to wild-type mice. This indicated that intrinsic S100A8/A9 has no effect on

osteoclastogenesis. In contrast, recombinant S100A8 adding to the culture of osteoclast precursors enhanced osteoclast differentiation and function in dose-dependent manner. In addition, extrinsic S100A8 also affect the organization of osteoclast cytoskeleton. These effects of S100A8 were mediated by TLR-4 but not RAGE. In contrast to S100A8, S100A9 or heterodimer of S100A8/S100A9 did not affect the differentiation and function of osteoclasts [94].

Chapter 3

Materials and Methods

Culture of hDPCs

HDPCs were obtained from caries-free lower third molars using explant method [34, 95]. Briefly teeth were split using hammer and the pulp tissue were collected, cut into pieces and placed in cell culture dishes to allow the outgrowth of the cells from dental pulp fragments (Figure 12). The culture media used was Dulbecco's modified Eagle's medium (DMEM) (GIBCO, ThermoFisher Scientific, NY, USA) supplemented with 10% fetal bovine serum (GIBCO), 2 mM L-glutamine, 100 U/mL penicillin, 100 mg/mL streptomycin, and 0.25 µg/mL Amphotericin B (GIBCO). The cells were cultured in a humidified atmosphere with 5% CO_2 at 37 °C and expanded until 3rd to 6th passage before used for mechanical force application. When using for force application, cells were then seeded on 6-well plate at the density of 300,000 cells/well overnight. Three hours prior to force application, cells were starved in serum-free media and the media was changed again just before force application.

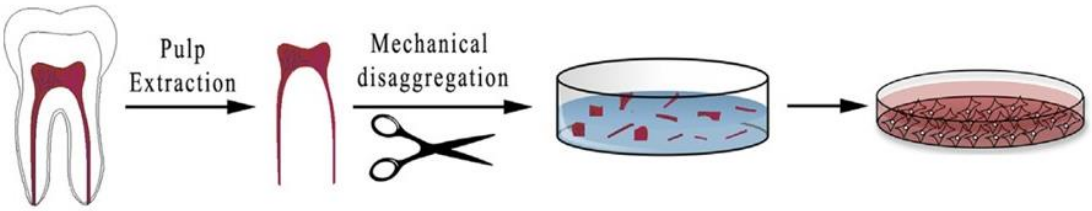

Figure 12 Obtaining hDPCs by explant method. Dental pulp collected from teeth were disaggregated and placed into cell culture dish to allow the outgrowth of hDPCs (picture from La Noce et al [95])

Culture of hPDLs

HPDLs were also obtained from caries-free lower third molars by explant method. Briefly, PDL tissue was scraped from the teeth and placed in tissue culture dish

supplement with the cell culture media as in culture of hDPCs. Cells were expanded until 3rd to 6th passage to be used for force application.

Mechanical force application models

Metal weight compressive force application model

In this mechanical stress model, the compressive force was generated by placing a plastic cylinder containing metal coins over the media covering cell layer in 6-well plate (Figure 13). The plastic cylinder used had the diameter that was fit to the culture well. The force level was calculated by dividing the total weight applied (weight of coins, plastic cylinder and media) by the area culture well. The force level can be adjusted by varying the weight of metal coins put in the plastic cylinder. The plastic cylinder with the metal coins fixed in were then gently placed onto the media covering cell layer to produce the determined compressive force level (Figure 13). This method of force application was previously used by many study [34, 35, 96, 97].

Figure 13 Metal weight compressive force application model. (A) Diagram showing how force was applied to the cells in this model. (picture from Kanzaki et al [96]). (B) the metal coins of various weight were used to produce various force level to the cells. C. The metal coins were fixed to the plastic cylinder and gently placed onto the media covering cell layer. D. The cells subjected to mechaical force and control cells without force application.

Computerized compressive force application model

This model utilized a compressive force apparatus introduced and described in details in the study of Manokawinchoke *et al* [98]. The main components of the apparatus that generate the compressive force are the pestles and the cylinders. Briefly, the desired compressive load is set using a computer software. The 6-well culture plate with cell layer plated will be attached to the cylinders. The computer-controlled motor will drive the culture plate and the cylinders up toward the pestles until the pestle submerge into the medium in the culture plate. The compressive force is thus generated by the increase in hydrostatic pressure at the bottom of the culture plate. The balance attached under the culture plate will show the weight generated and send the signal back to the controller so that the force can be monitored (Figure 14). This model can produce static as well as intermittent compressive force and was used in previous studies of Manokawinchoke *et al* [98] and Peetiakarawach *et al* [99].

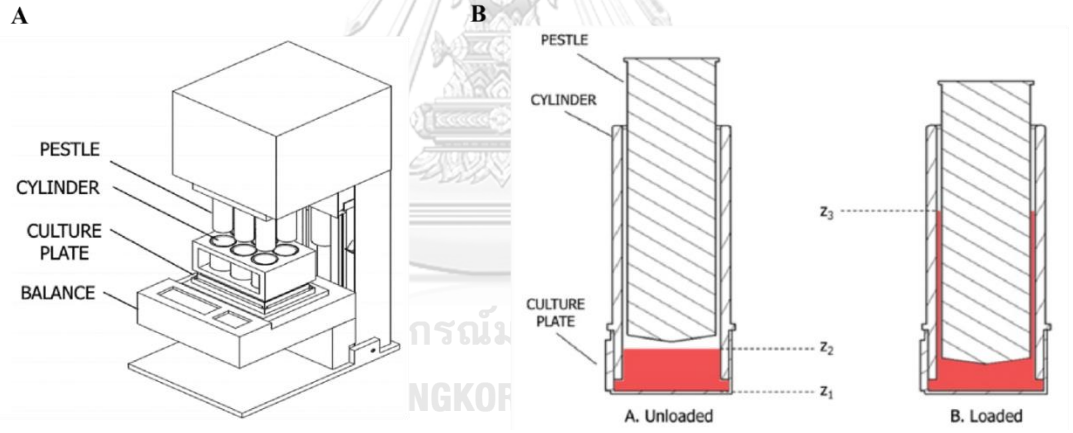

Figure 14 Computerized compressive force application model. (A) The compressive force apparatus used with 6-well plate. (B) The pestle and cylinder when unloaded and loaded. (Picture from Manokawinchoke et al [98])

Cell viability assay

Cell viability was determined as the following steps.

1. 0.5 mg/mL of 3-(4,5-dimethylthiazol-2-yl)-2,5-diphenyltetrazolium bromide) (MTT; Life technologies, ThermoFisher Scientific, OR, USA) solution was prepared in culture media without phenol red.

2. The culture media in cell culture wells was removed and cells were washed once with phosphate buffer saline (PBS)
3. Cells were incubated with 0.5 mg/mL 3-(4,5-dimethylthiazol-2-yl)-2,5-diphenyltetrazolium bromide solution (MTT; Life technologies, ThermoFisher Scientific, OR, USA) in the dark, at 37^{o}C with 5% CO_2 for approximately 30 min.
4. Formazan crystals were dissolved in a detergent solution containing 1:9 dimethyl sulfoxide (DMSO; AMRESCO, OH, USA) and glycine buffer (0.1 M glycine/0.1 M sodium chloride pH 10).
5. The solution was then measured for the absorbance at 570 nm using microplate reader (ELx800; BIO-TEK®, VT, USA).

Collecting of dental pulp tissue from premolar teeth of orthodontic patients

Premolars extracted from orthodontic patients before or after 3-6 months following orthodontic treatment were kept in DMEM. The teeth were split with hammers and fresh pulp tissue was collected and further used for analysis of gene expression.

Quantification of gene expression

Extraction of total RNA

Total RNA from of cultured hDPCs and osteoclasts as well as from dental pulp tissues collected from premolar teeth were extracted using TRIzol™ (Invitrogen, ThermoFisher Scientific) reagent following these steps.

1. Adding TRIzol™
   1.1 In cultured cells, culture media in culture wells was discarded wash with dPBS once. The TRIzol™ was then added into each culture well and left for 5-10 minutes before transferring the solution into 1.5 ml tube.
   1.2 In dental pulp tissue, the pulp tissue was minced into small fractions using RNase free instruments and transferred to 1.5 ml tube. The TRIzol™ was then added into 1.5 ml tube containing pulp tissue.

2. Chloroform (Sigma-aldrich, MO, USA) was then added and the solution was homogenized.
3. Solution was allowed to separate into layers and was centrifuged at 12000g for 15 minutes at 4°C for complete separation.
4. The upper aqueous layer which contains RNA was collected into 1.5 ml tube and was precipitate by adding isopropanol for at least 2 hours.
5. The RNA containing solution was then centrifuged at 12000g for 15 minutes at 4°C to collect RNA pellet.
6. Isopropanol supernatant was then discarded and re-suspended with 75% ethanol and was centrifuge at 7000g for 5 minutes.
7. Ethanol supernatant was then completely discarded.
8. RNA pellet was dissolved with RNase-free water
9. The amount of RNA obtained was measured using a spectrophotometer (NanoDrop2000, Thermo Scientific).

Synthesis of complementary DNA (cDNA)

The 1 µg of the RNA was used for complementary DNA (cDNA) synthesis by iScript™ Reverse Transcription Supermix for RT-qPCR (Bio-RAD, CA, USA) following manufacturer's protocol. Briefly, each reaction volume was 20 µl composed of 4 µl of iScript RT Supermix, and 1 µg of the RNA sample in 16 µl of nuclease-free water. The reaction mix was incubated for 5 minutes at 25ºC, 20 minutes at 46ºC and 1 minutes at 95ºC in thermocycler (PCR GeneAmp 9700; Applied Biosystems)

Real-time polymerase chain reaction (PCR)

Real-time quantitative PCR was performed using iTaq™ Universal SYBR® Green Supermix in LightCycler® 480 II (Roche, Basel, Switzerland) following manufacturer's protocol. Briefly, the reaction volume used was 10 µl composing of 5 µl of iTaq™ Universal SYBR® Green Supermix, 0.5 µl of 10 µM forward primer, 0.5 µl of 10 µM reverse primer and 4 µl of water containing cDNA sample. The primers were prepared following the reported sequences from GenBank as listed in Table 3. Expression of target gene was normalized to internal control, *GAPDH* gene. The

cycling parameters were as the follow: pre-incubation at 95°C for 5 min, followed by 40 cycles at 95°C for 10 s, 60°C for 10 s and 72°C for 30 s.

Table 3 The list of primers used in this study

Gene	Primer Sequences (5' to 3')
GAPDH	Forward- CACTGCCAACGTGTCAGTGGTG
	Reverse- GTAGCCCAGGATGCCCTTGAG-R
IL6	Forward-ATGCAATAACCACCCCTGAC
	Reverse-AAAGCTGCGCAGAATGAGAT
IL1B	Forward-GCAGAAGTACCTGAGCTCGC
	Reverse-CTTGCTGTAGTGGTGGTCGG
VEGF	Forward-ATGAGGACACCGGCTCTGACCA
	Reverse-AGGCTCCTGAATCTTCCAGGCA
S100A7	Forward-GATTGACAAGCCAAGCCTGC
	Reverse-CAAAGACGTCGGCGAGGTAA
S100A4	Forward-GAACTAAAGGAGCTGCTGACCC
	Reverse-TTCATCTGTCCTTTTCCCCAA
S100A8	Forward-AAGCTGTCTCTGATGGCCTG
	Reverse-GTCAACATGATGCCCACGGA
EGF	Forward -CTGGAGCTGTCCTGAAGGTA
	Reverse-TAAAGGCTTCCAGCCACCTC
EGFR	Forward -AAGTGTGATCCAAGCTGTCC
	Reverse-CCGTGATCTGTCACCACATA
NOTCH1	Forward -GCCGCCTTTGTGCTTCTGTTC
	Reverse-CCGGTGGTCTGTCTGGTCGTC
NOTCH2	Forward -CCAGAATGGAGGTTCCTGTA
	Reverse-GTACCCAGGCCATCAACACA
NOTCH3	Forward -TCTTGCTGCTGGTCATTCTC
	Reverse-TGCCTCATCCTCTTCAGTTG
NOTCH4	Forward -AGCCGATAAAGATGCCCA
	Reverse-ACCACAGTCAAGTTGAGG

Table 3 (Continued) The list of primers used in this study

Gene	Primer Sequences (5' to 3')
HES1	Forward -AGGCGGACATTCTGGAAATG
	Reverse-CGGTACTTCCCCAGCACACTT
HEY1	Forward -CTGCAGATGACCGTGGATCA
	Reverse-CCAAACTCCGATAGTCCATAGCA
RAGE	Forward -CCAACTACCGAGTCCGTGTC
	Reverse-CCGTGAGTTCAGAGGCAGAA
RANK	Forward -CTGTGGCCCGGATGAATACT
	Reverse-CAGGGCCTTGCCTGTATCAC

Quantification of protein expression

The concentration of S100A7 protein was determined by S100A7 ELISA kit (CircuLex, MBL, Nagoya, Japan) following manufacturer's recommendation as the following steps.

1. One-hundred µl of the samples and the series of S100A7 standard solutions were added into the microtiter wells and incubated for 2 hours at room temperature.
2. The wells were washed 4 times with Wash buffer following by adding 100 µl of Horseradish peroxidase (HRP) conjugated Detection Antibody into each well and incubated in room temperature for 1 hour.
3. The well were them washed 4 times and 100 µl of Substrate Reagent was added into each well and incubated at 37°C in dark for 30 minutes.
4. The Stop Solution were added into each well in the same order as the Substrate.
5. The optical absorbance at 450 nm was measured using microplate reader (ELx800; BIO-TEK®).

Culture of osteoclasts

Obtaining of osteoclast precursors

Osteoclast precursors were obtained from $CD14^+$ fraction of PBMC of healthy subjects following these steps. PBMC were separated by density centrifugation using Histopaque (Sigma-aldrich), and $CD14^+$ monocytes were enriched using human CD14 microbeads (Miltenyi Biotec, CA, USA) following these steps.

1. Fifty milliliters of the peripheral/venous blood was collected from each of healthy donor and stored in anticoagulant coated vessels.
2. Blood sample was diluted blood 1:1 v/v with RPMI 1640 (GIBCO)
3. The diluted blood samples of 25 ml each was then gently pipetted into 50 ml tubes filled with 12.5 ml of Histopaque to allow the blood sample to suspend on the Histopaque layer before centrifugation for 30 minutes at 900 g, no brake at room temperature.
4. PBMC fraction was then collected and transferred into a new tube using a sterile plasture pipette
5. PBMCs were then washed 1 ml FBS together with RPMI medium with the volume at least twice the volume of PBMC fraction obtained. After centrifugation for 10 minutes at 1200 rpm the supernatant was discarded and PBMCs was resuspended in buffer containing BSA and EDTA prepared for cell separation using magnetic-activated cell sorting (MACS) system recommended by manufacturer.
6. The PBMCs obtained were the counted and ratio was adjusted to 10^7 cells/80 µl and were incubated with CD14 microbeads at the ratio of 10^7 cells/20 µl of microbeads for 30 minutes at 4°C.
7. The unbound microbeads were then washed with 1.5 ml of buffer per 10^7 cells. After centrifugation at 300g for 10 minutes, the supernatant was discarded and cells were resuspended n 500 µl of buffer.
8. The cells suspension was then passed through the column attached to magnetic field to allow $CD14^+$ cells (monocytes) to attach to the column while $CD14^-$ cells passing out (Figure 15).

9. The magnetic field was then removed and monocytes were then eluted and use as the precursors of osteoclasts.

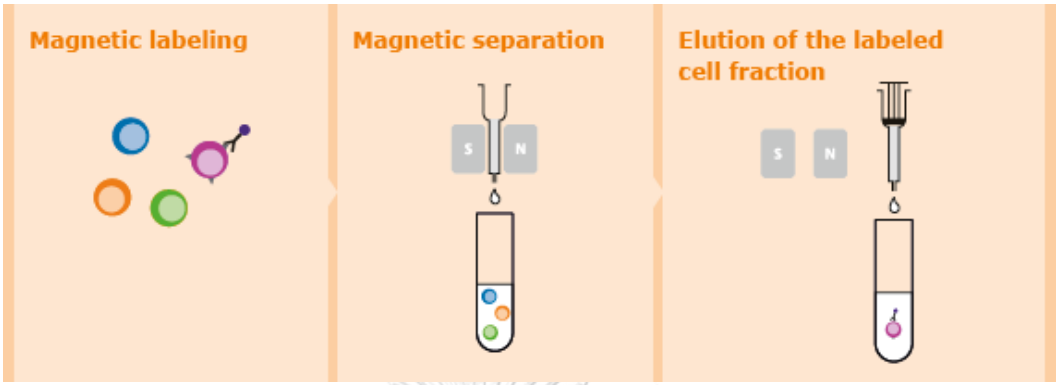

Figure 15 Diagram illustrates cell separation using magnetic-activated cell sorting (MACS) system. (Picture from http://www.miltenyibiotec.com)

Cell density, media used and culture duration

For determination of number of $TRAP^+$ cell, 10^5 of $CD14^+$ monocytes were plated in each well of 96-well plate supplement with 200 µl of media. For determination of gene expression, $3x10^5$ of monocytes were cultured in 48-well plate supplement with 500 µl of media. For detection of resorptive activity, $3x10^5$ cells in 20 µl of media were seeded onto 8 mm-in-diameter dentin slice placed in 48-well plate for 20-30 minutes before the media was further added to obtain the volume of 500 µl.

The media used were α-MEM (HyClone, UT, USA) supplemented with 10% FBS (Certified, US origin, GIBCO), 0.2 mM Glutamax (GIBCO), 100 U/mL penicillin, 100 mg/mL streptomycin (GIBCO), and 0.25 µg/mL Amphotericin B (GIBCO), 25 ng/ml recombinant human (rh) RANKL (Peprotech) and 25 ng/ml rhM-CSF (Peprotech, NJ, USA) in a humidified atmosphere with 5% CO2 at 37 °C. The culture media were changed every 2-4 days and the cells were cultured for 4 or 7 days before total RNA was collected or for 14 days before cells were stained with TRAP for investigation of osteoclast number or dentin slices were collected for investigation of resorption pit.

Determination of osteoclast number

Cell were fixed in 10% (v/v) formalin for 10 min and washed in 95% (v/v) ethanol. Cell were then stained for TRAP with 0.1 mg/ml naphthol AS-MX phosphate (Sigma-Aldrich) and 0.5 mg/ml fast red violet LB salt (Sigma-Aldrich) in 50 mM sodium acetate buffer, pH 5.0, containing 50 mM sodium tartrate, for 20 minutes. The TRAP-positive cells were observed under a bright field microscopy (Olympus BX50, Tokyo, Japan) and imaging processor (Olympus DP72, Tokyo, Japan) with 100x stage objectives. The number of TRAP-positive cells were counted from at least 3 fields per sample. The total number of osteoclast were calculated as the fold change compared to control condition.

Determination of pit resorption

Dentin slices were collected form the culture and cells on dentin slices were removed by sonication in 25% Ammonium Hydroxide for 1 minute. After washing with water for 4 times, dentin slices were then stained with 1 mg/ml Toluidine Blue for 1 minute. Resorption pits were visualized under a bright field microscopy (Olympus BX50) and imaging processor (Olympus DP72) with 100x stage objectives. The photographs were taken from 3 fields of each dentin slice. Area of resorption were measured using polygonal measurement tool of CellSens software (Olympus). The total area of resorption in each sample was compared to the total area of resorption in control condition and calculated as fold change.

Ethical consideration

The study protocols regarding collecting pulp tissue from patient's teeth and collecting peripheral blood from volunteers were approved by the Human Research Ethics Committee, Faculty of Dentistry, Chulalongkorn University (HREC-DCU 2017-069) and the procedure was performed according to the Declaration of Helsinki.

Experimental design

Comparison of *in vitro* mechanical force application models

HDPCS were subjected to mechanical force of 2 g/cm^2 for 2 hours by both models of mechanical force application. HDPCs not receiving any force culturing in the same duration were served as control for each models of force application. *IL6* and *OCT4* gene expression was determined (Figure 16). The level of gene expression was further calculated as the fold changes compared to control in each line of hDPCs.

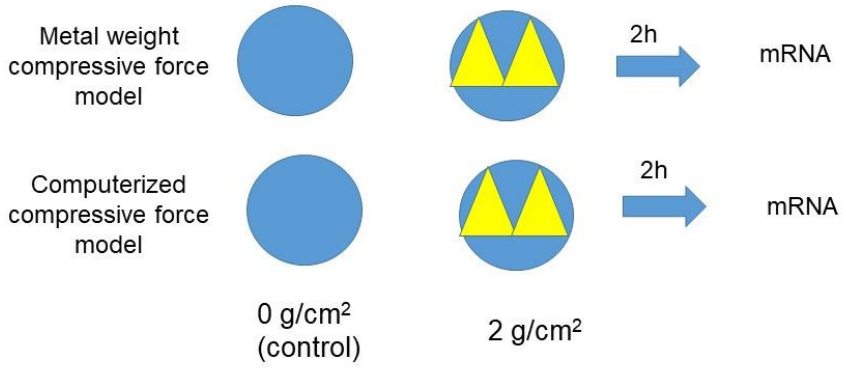

Figure 16 The diagram showing the experimental design for comparison of mechanical force application models

Determination of cell viability and inflammatory cytokine expression

HDPCS were subjected to mechanical force of 2 g/cm^2 for 6 hours by metal weight compressive force application that were used in all of the following compressive force experiments. HDPCs not receiving any force culturing in the same duration were served as control. Cell viability and expression of inflammatory cytokine genes, *IL6*, *IL1B* and *VEGF* was determined (Figure 17). The level of inflammatory cytokines mRNA expression was further calculated as the fold changes compared to control in each line of hDPCs.

Determination of the changes in S100 mRNA expression following *in vitro* mechanical stress application

HPDCs and hPDLs were subjected to mechanical force of different magnitude (1 and 2 g/cm^2) and duration (2 and 6 hours). HDPCs and hPDLs not receiving any

force culturing in the same duration were served as control. *S100A7*, *S100A4* and *S100A8* mRNA expression was determined (Figure 18). The level of mRNA expression was further calculated as the fold changes compared to control in each line of hDPCs and hPDLs.

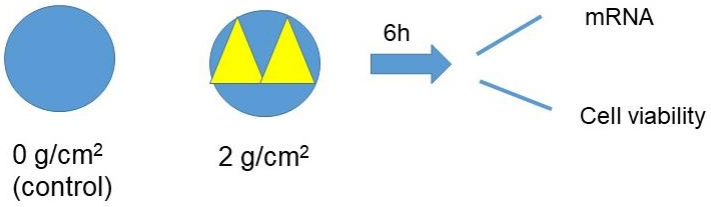

Figure 17 The diagram showing the experimental design for determination of cell viability and inflammatory cytokines expression in hDPCs subjected to mechanical stress

Determination of *S100A7* mRNA expression in dental pulp following *in vivo* mechanical stress application

Premolars teeth obtained from the group of orthodontic patients who have their premolars extracted before orthodontic treatment or from the other group of patients having their premolars extracted 3-6 months following orthodontic treatment. Premolars extracted from the group of orthodontic patients before orthodontic treatment were served as control. S100A7 mRNA expression in dental pulp tissue of these control and orthodontically moved teeth was determined and compared.

Determination of the S100A7 protein secreted from hDPCs

HDPCs were subjected to mechanical force of 1 and 2 g/cm^2 for 2 and 6 hours. HDPCs not receiving any force culturing in the same duration were served as control. S100A7 protein level was measured (Figure 19).

Determination of other genes implicated in mechanical stress-induced S100A7

HDPCs were subjected to mechanical force of 1 and 2 g/cm^2 for 2 hours. HDPCs not receiving any force culturing in the same duration were served as control.

Expression of *EGF*, *EGFR*, *NOTCH1-4*, *HES1* and *HEY1* genes was determined (Figure 20). The level of mRNA expression was further calculated as the fold changes compared to control in each line of hDPCs.

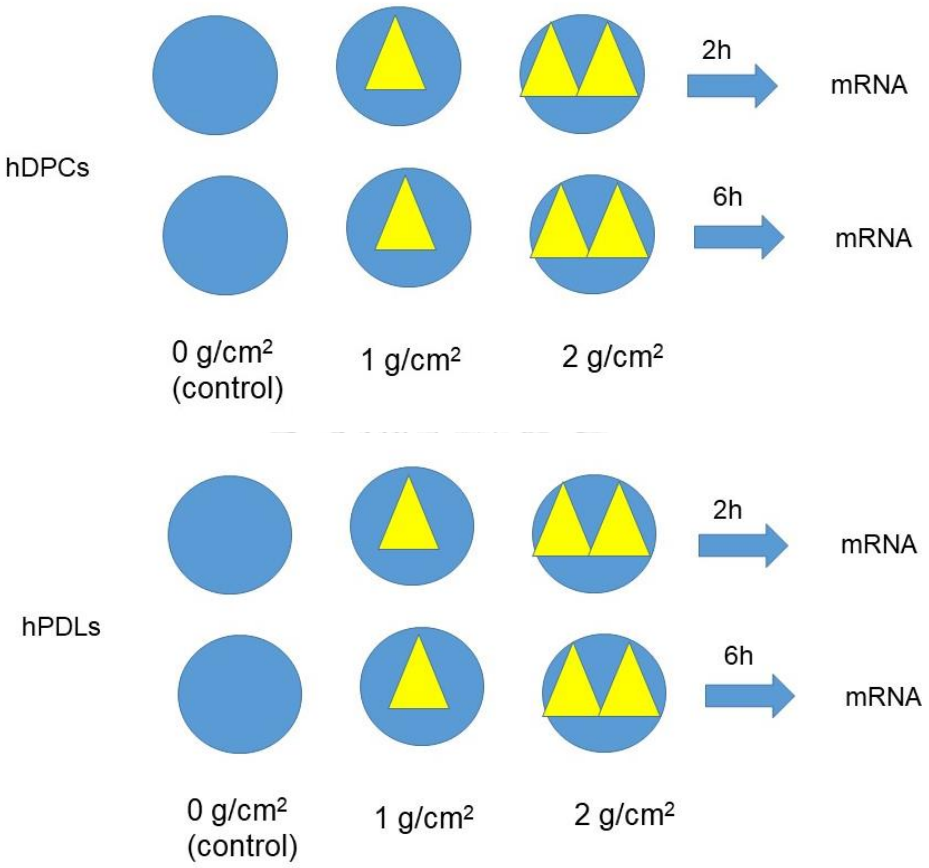

Figure 18 The diagram showing the in vitro experimental design for investigation of changes in S100 mRNA expression in hDPCs and hPDLs following in vitro mechanical stress application.

Investigation of the effect of S100A7 on osteoclast differentiation and function

The effect of S100A7 on osteoclastogenesis was determined using rhS100A7. Human osteoclast precursors were differentiated into osteoclasts in the presence of varying concentration of recombinant rhS100A7. Osteoclasts precursors differentiated in the absence of recombinant S100 were served as control. The number of osteoclast and area of resorption was determined (Figure 21). The number of osteoclast and area

of pit resorption was further calculated as ratio compared to control cells from each line of precursors.

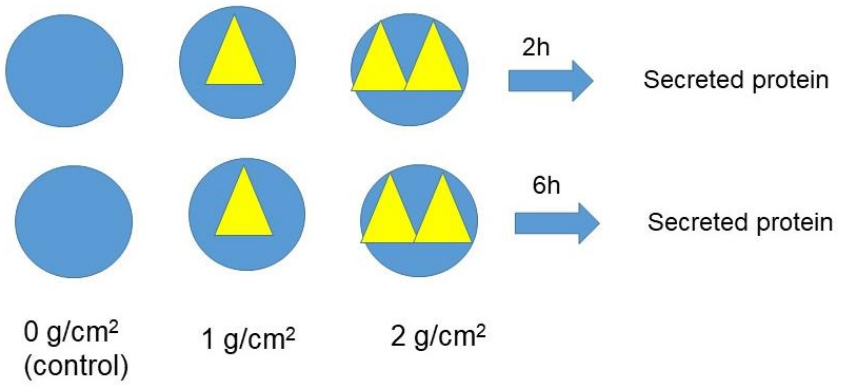

Figure 19 The diagram showing the in vitro experimental design for investigation the secreted S100A7 in hDPCs subjected to mechanical stress.

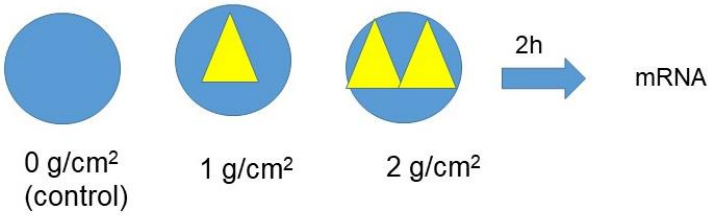

Figure 20 The diagram showing the in vitro experimental design for investigation other related genes.

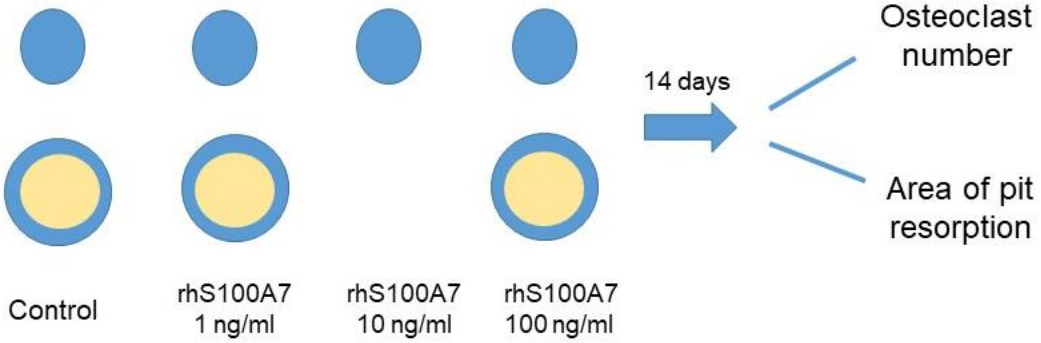

Figure 21 Diagram showing experimental design to determine the effect of S100A7 on osteoclast differentiation and function

Investigation of the effect of S100A7 on osteoclast differentiation with or without RANKL and M-CSF

Osteoclast precursors were differentiated into osteoclasts in the presence or absence of either RANKL or M-CSF, with or without 100 ng/ml rhS100A7. Osteoclast precursors were also differentiated in the presence both RANKL, M-CSF and 100 ng/ml rhS100A7. Control groups were the precursors stimulated with RANKL and M-CSF (Figure 22). The osteoclast number was determined and further calculated as ratio compared to control cells from each line of precursors.

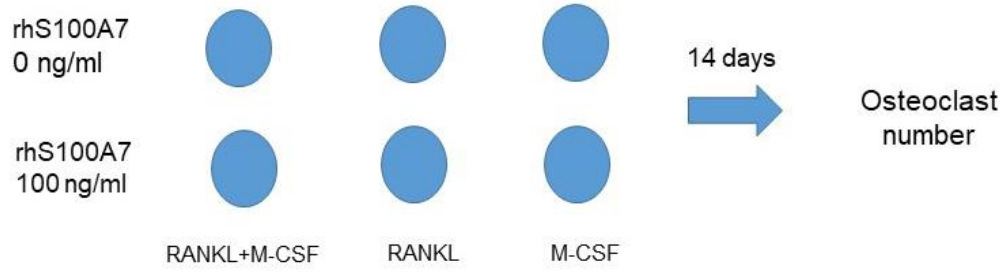

Figure 22 Diagram showing experimental design to determine the effect of S100A7 on osteoclast differentiation with and without RANKL or M-CSF

Investigation of the effect of S100A7 on expression of RAGE and RANK during osteoclastogenesis

Osteoclast precursors were differentiated in osteoclast media supplement with rhS100A7 of 0 ng/ml (control) or 100 ng/ml for 4 and 7 days. Expression of *RAGE* and *RANK* mRNA was determined (Figure 23).

Data Analysis

Student T-test was used to compare the mean fold change of mRNA, mRNA level, protein level, number of osteoclast and area of pit resorption between each experimental group and the control group with the confidence interval of 95%.

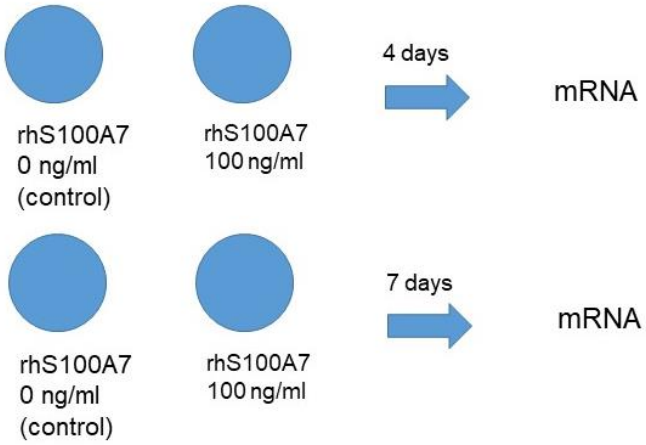

Figure 23 Diagram showing experimental design to determine the effect of S100A7 on expression of RAGE and RANK during osteoclastogenesis

Chapter 4

Results

Validation of *in vitro* mechanical stress model

Comparison between two models of mechanical stress on the response of hDPCs

Previous study by Satrawaha *et al* [34] found that there was the upregulation of IL-6 in hDPCs subjected to mechanical stress using the metal weight compressive force model. The same compressive force model was also used to apply mechanical force to SHED [35]. In these previous studies, inflammatory cytokines genes including *IL6* and the stem cell marker genes including *OCT4* was found upregulated following mechanical force application [34, 35]. Recently, the computerized compressive force model was developed [98]. Therefore, in the first part of this study, both models of mechanical stress were applied to hDPCs of two independent lines and the expression of *IL6* and *OCT4* gene was investigated using real-time PCR.

OCT4 was found upregulated in one line of hDPC while relatively unchanged in the other line (Figure 24A). However, when comparing between the use of mechanical stress of both model in the same line of hDPCS, the expression of *OCT4* was comparable between two models of mechanical stress application (Figure 24A). *IL6* was upregulated following mechanical stress application in both lines of hDPC using both models of mechanical force application (Figure 24B). These results suggested that although there were some variations in response of hDPCs of different lines, in the same line of hDPCs used, both models of mechanical force application could produce the same response of hDPCs.

Effect of *in vitro* mechanical force application on cell viability and inflammatory response of HDPCs

Since two mechanical stress models produce comparable response of hDPCs. The metal weight compressive force application was selected to further used in this

study because this model is more convenient to applied continuous force with varying force magnitude and duration in the same experiment.

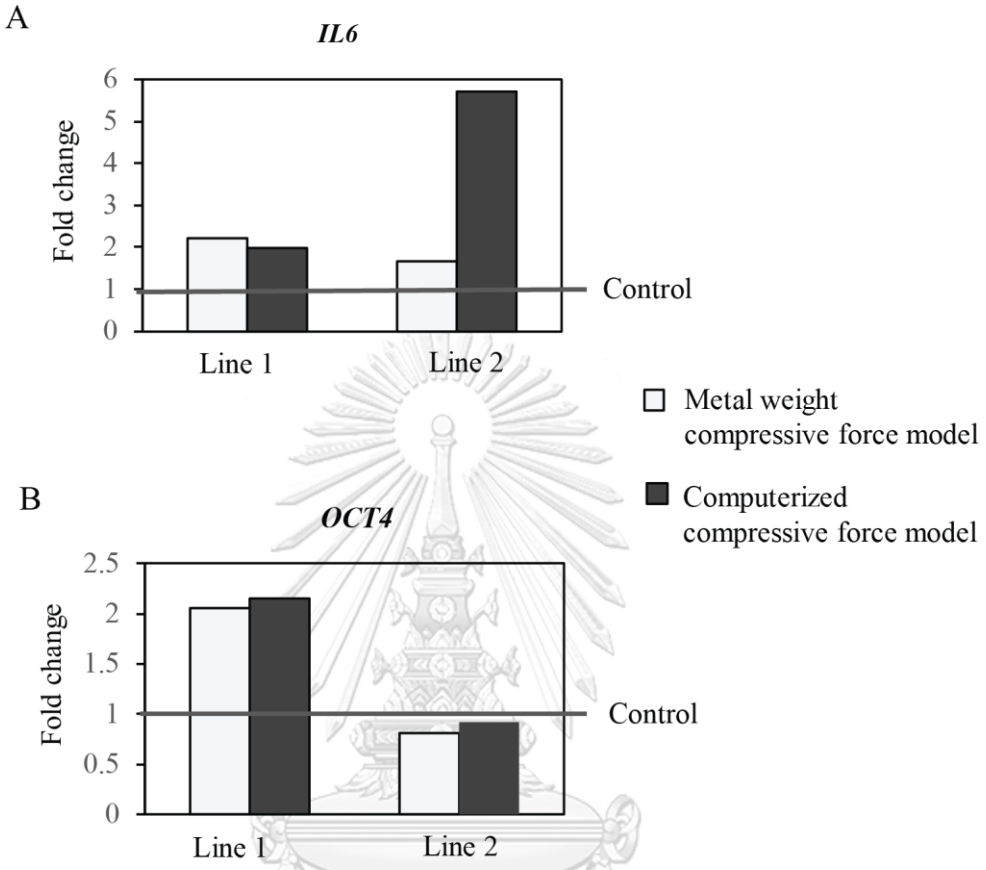

Figure 24 Expression of IL6 and OCT4 genes in 2 lines of hDPCs subjected to mechanical loading of 2 g/cm^2 for 2 hours using two models of mechanical stress

To further verify this *in vitro* mechanical force model, cell viability was determined. HDPCs were subjected to mechanical loading of 0 g/cm^2 (control) or 2 g/cm^2 for 6 h. Cell viability reflected by the absorbance measured following MTT assay was not statistically different between hDPCs subjected to mechanical loading and control hDPCs (Figure 25). This result indicated that mechanical loading using this model did not affect viability of hDPCs.

Expression of inflammatory mediators were also determined following mechanical loading. Inflammatory cytokines, *IL1B*, *IL6* and *VEGF* gene was significantly up-regulated in hDPCs subjected to mechanical loading of 2 g/cm^2 for 6

hours compared to control hDPCs (Figure 26). Altogether, these results indicated that mechanical loading did not affect cell viability while inducing the inflammatory response of hDPCs.

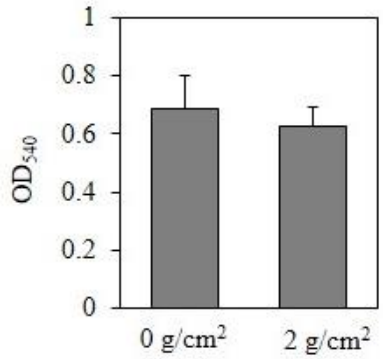

Figure 25 Viability of hDPCs subjected to mechanical loading compared to control. The absorbance at 540 nm measured immediately after MTT assay indicated the viability of hDPCs subjected to mechanical loading and no force control for 6 hours. Values are presented as mean ± standard deviation (n=4).

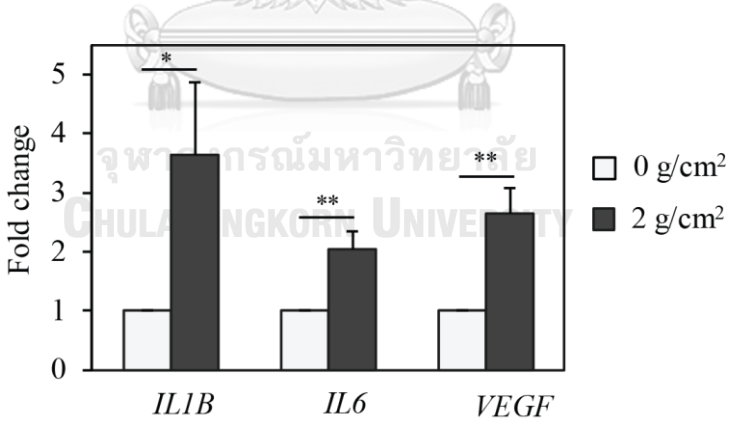

Figure 26 Expression of IL1B, IL6 and VEGF genes in hDPCs subjected to mechanical loading compared to control at 6 hours. Values are presented as mean ± standard deviation (n=3). *p<0.05, **p<0.01.

Induction of S100A7 in mechanical stress-induced hDPCs

Expression of *S100A7* genes in hDPCs following in vitro mechanical loading

Expression of *S100A7* mRNA expression in hDPCs following mechanical stress challenging was investigated, first, using in vitro mechanical force application model. *S100A8* and *S100A4* was also investigated. S100A8 is one of well-known DAMPs that was reported to have stimulatory effect on osteoclast. S100A4 was reported to up-regulated in hDPLs receiving mechanical force and also have been reported to enhance osteoclast differentiation.

HDPCs subjected to mechanical loading of 1 and 2 g/cm^2 for 2 hours significantly increased expression of *S100A7* mRNA compared to control (Figure 27A). At 6 hours after mechanical loading, no difference in *S100A7* gene expression was observed between hDPCs receiving mechanical loading and control hDPCs. Expression of *S100A4* and *S100A8* gene was not significantly different between hDPCs subjected to mechanical loading of both magnitudes and durations (Figure 27B and Figure 27C). These results suggested the selective up-regulation of *S100A7* by hDPCs in early response to mechanical loading.

Expression of S100 genes in hPDLs following in vitro mechanical loading

Expression of *S100A7*, *S100A4* and *S100A8* in hPDLs subjected to mechanical stress was also investigated to compare the mechanical stress-induced expression of *S100* genes between hPDLs and hDPCs.

Expression of *S100A7* gene did not significantly change after applying mechanical loading to hPDLs (Figure 28A) while this gene was up-regulated following mechanical loading in hDPCs (Figure 27A). No changes in *S100A4* gene expression was observed hPDLs as well as hDPC except for 2 g/cm^2 for 6 hours that hPDLs showed significantly downregulation of *S100A4* (Figure 28B). *S100A8*, on the other hand, was significantly up-regulated in hPDLs subjected to mechanical force both of 1 and 2 g/cm^2 for 2 hours (Figure 28C) while no significant change in *S100A8* was found in hDPCs subjected to mechanical loading (Figure 27C).

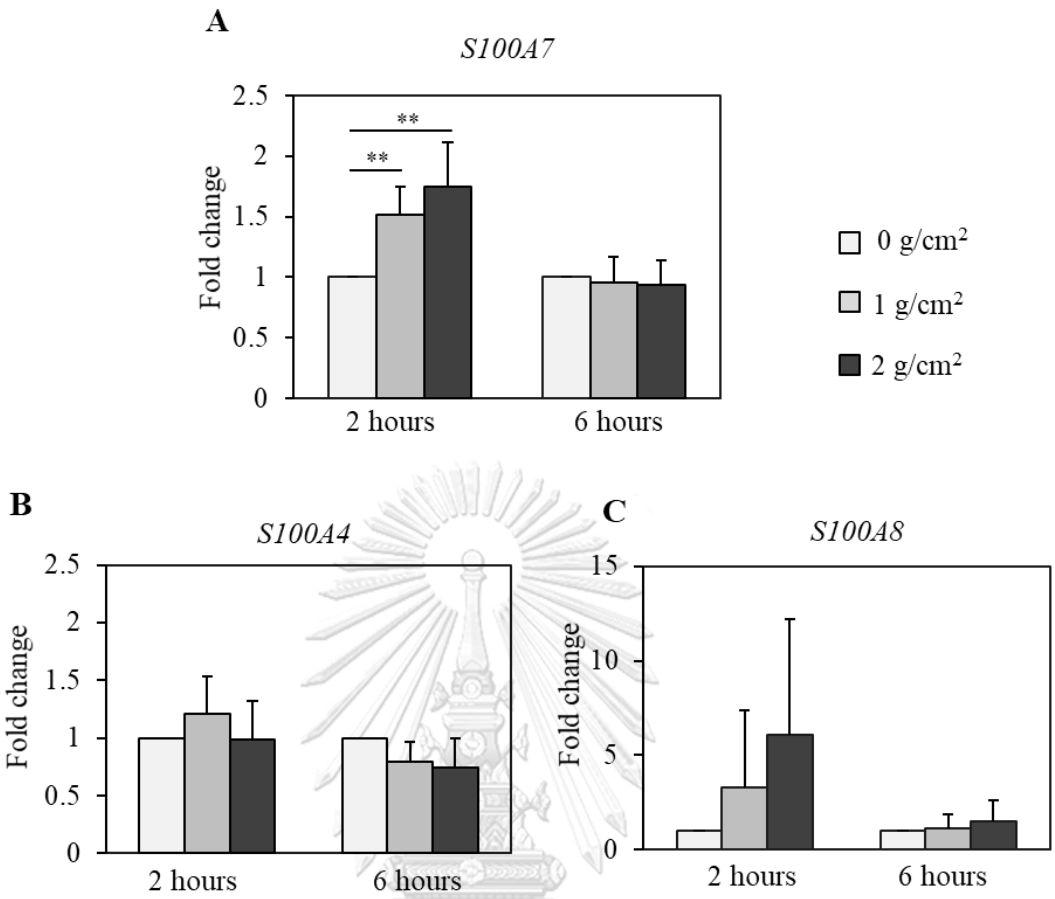

Figure 27 Expression of (**A**) S100A7, (**B**) S100A4 and (**C**) S100A8 genes in hDPCs subjected to mechanical loading compared to control hDPCs. Values are presented as mean ± standard deviation (n=4). **p<0.01

These results suggested that, in response to mechanical stress, hPDLs and hDPCs differently expressed *S100* genes. HPDLs up-regulated *S100A8* in response to mechanical stress while *S100A7* was the main *S100* gene up-regulated in hDPCs in following mechanical stress challenging.

Expression of *S100A7* genes in human dental pulp tissue following *in vivo* mechanical loading

To confirm the expression of *S100A7* following mechanical loading of hDPCs in vivo, orthodontic treatment was selected as the representative model of the mechanical stress. Total mRNA from pulp tissue was collected from premolars extracted before (control) or after orthodontic force was applied. The results showed

that *S100A7* gene was significantly up-regulated in dental pulp of orthodontically moved teeth compared to control teeth without orthodontic force application (Figure 29). This result confirmed the in vitro results that *S100A7* was up-regulated in human dental pulp in response to mechanical stimuli.

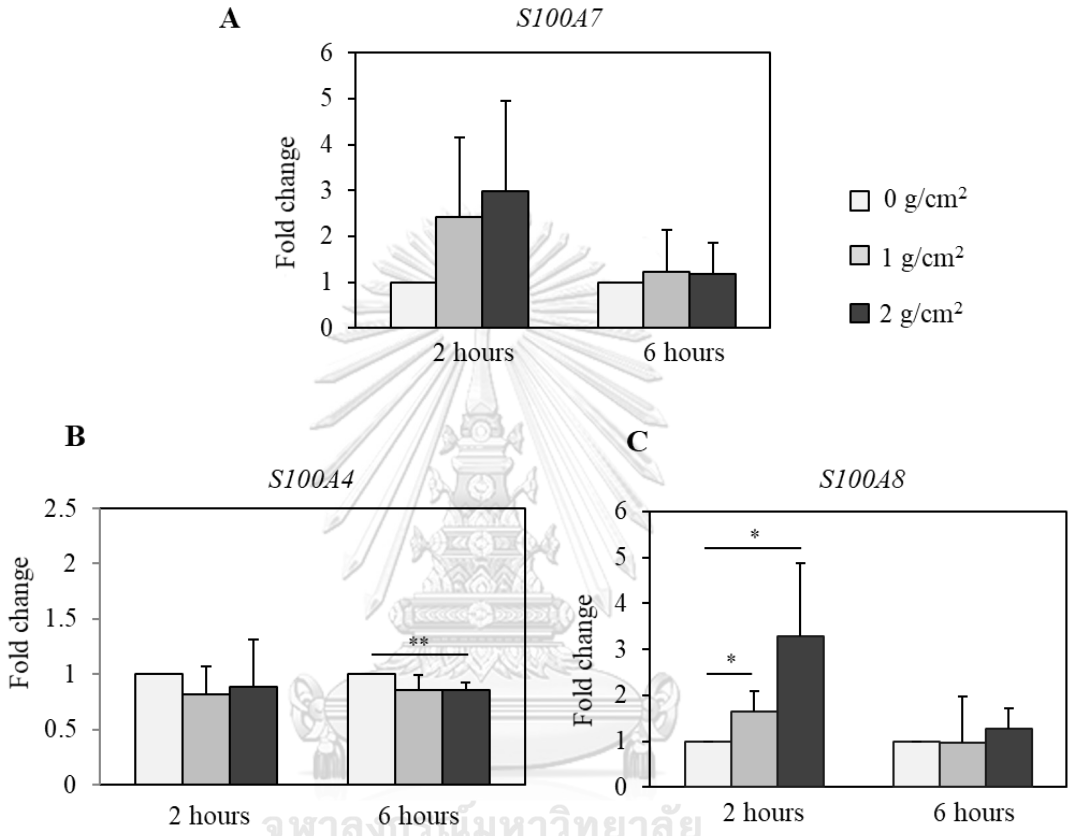

Figure 28 Expression of (**A**) S100A7, (**B**) S100A4 and (**C**) S100A8 genes in hPDLs subjected to mechanical loading compared to control hPDLs. Values are presented as mean ± standard deviation (n=4). *p<0.05, **p<0.01

Secretion of S100A7 protein following in vitro mechanical loading of hDPCs

S100A7 can act as cytokines releasing from the cells to have the effect on other cells. The secretion of S100A7 protein following mechanical stress was investigated. At 2 hours after mechanical loading, there was no significantly difference in S100A7 protein concentration in supernatant between control hDPCs and hDPCs subjected to mechanical loading (Figure 30). The significantly higher concentration of S100A7

protein was observed in supernatant of hDPCs subjected to both 1 and 2 g/cm^2 mechanical loading at 6 hours following the mechanical loading (Figure 30). These results suggested that following the up-regulation of *S100A7* mRNA expression, S100A7 protein was also secreted from hDPCs in response to mechanical stress.

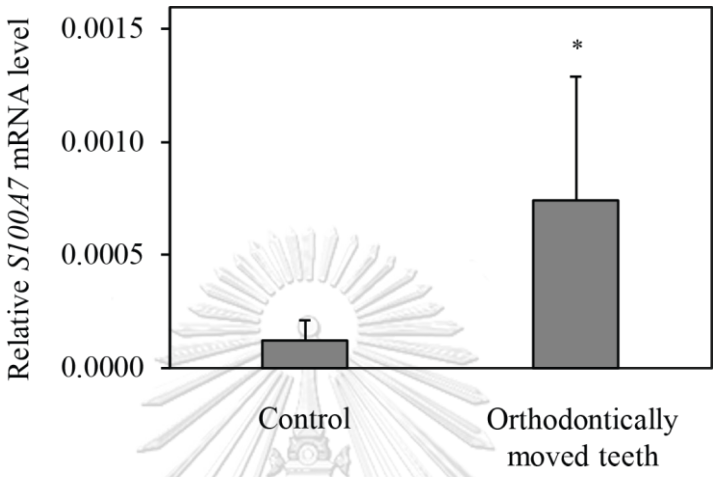

Figure 29 Expression of S100A7 mRNA in dental pulp of orthodontically moved teeth compared to control teeth without orthodontic force application. Value are presented as mean ± standard deviation (n=6). *p<0.05

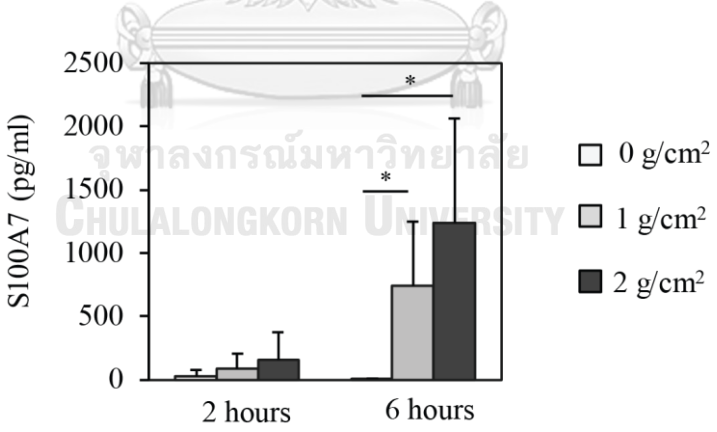

Figure 30 Concentration of S100A7 protein secreted by control hDPCs compared to hDPCs subjected to mechanical loading. Value are presented as mean ± standard deviation (n=4). *p<0.05

Effect of in vitro mechanical loading on *EGF* and *EGFR* mRNA expression

Since previous studies indicated that S100A7 can be induced by EFG/EGFR stimulation, the expression of *EFG* and *EGFR* following mechanical loading was also

determined. *EGFR* mRNA expression was not changed after hDPCs were stimulated with mechanical stress (Figure 31). However, there was a significant up-regulation of *EGF* following mechanical stress application of hDPCs at 2 g/cm^2 for 2 hours corresponding to the upregulation of *S100A7* mRNA expression (Figure 27). At 6 hours after mechanical stress application the *EGF* mRNA expression was significantly down-regulated (Figure 31).

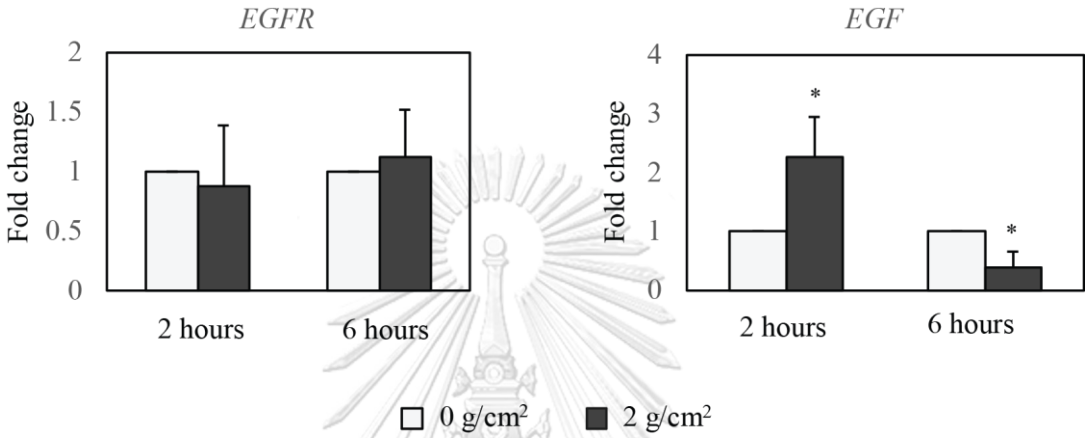

Figure 31 Expression of (**A**) EGFR and (**B**) EGF genes in hDPCs subjected to mechanical loading compared to control hDPCs. Value are presented as mean ± standard deviation (n=3). *p<0.05

Effect of in vitro mechanical loading on Notch receptors and target genes

Notch was reported to be implicated in psoriasis pathogenesis and notch signaling was also found related to dental pulp injuries. Therefore, notch and their target genes were investigated in hDPCs subjected to mechanical stress compared to control. After 2 hours of 2 g/cm^2 of mechanical force application, there was no significant change in mRNA expression of *NOTCH1*, *NOTCH3* and *NOTCH4* compared to control while *NOTCH2* was significantly down-regulated after mechanical force application (Figure 32A). Notch target gene, *HES1* was significantly up-regulated following mechanical stimuli, while *HEY1* mRNA expression was unchanged (Figure 32B). Up-regulation of *HES1* following mechanical stimuli suggested that there might be the stimulation of Notch signaling in hDPCs subjected to mechanical stress.

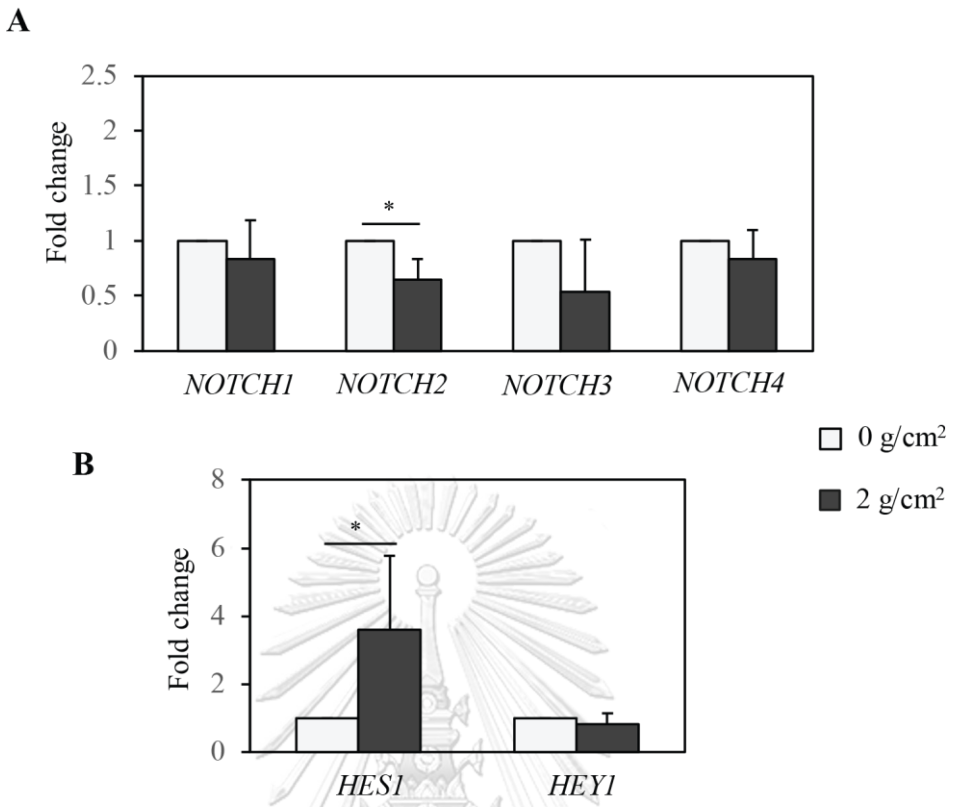

Figure 32 Expression of (**A**) NOTCH and (**B**) HES1 and HEY1 genes in hDPCs subjected to mechanical loading of 2 g/cm^2 compared to control hDPCs at 2 hours. Value are presented as mean ± standard deviation (A. n=3, B. n=5). *p<0.05

Effect of S100A7 on osteoclast differentiation and function

Effect of S100A7 on the number of osteoclasts and area of pit resorption

As the secretory S100A7 was detected in HDPCs subjected to the mechanical stress, the direct effect of this molecule on osteoclast differentiation was further investigated. Human CD14$^+$ monocytes were isolated and differentiated into osteoclasts in the absence or presence of rhS100A7 ranging from 1 ng/ml to 100 ng/ml. The TRAP$^+$ multinucleated cells were identified as the osteoclasts (Figure 33A). The number of osteoclasts was significantly increased in the presence of rhS100A7 in all concentration used, when compared to the control (Figure 33A and 33B).

Next, the effect of S100A7 on a bone resorption ability of osteoclasts was examined. Human CD14$^+$ monocytes were plated on dentine slices, and differentiated

into osteoclasts in the presence of 1 and 100 ng/ml of rhS100A7. The osteoclasts generated by rhM-CSF and rhRANKL, as a control, formed a number of pits (Figure 34A, control), which suggested that the cells were functionally active. The area of resorption pit was significantly increased in the presence of 1 and 100 ng/ml of rhS100A7 (Figure 34A and 30B). Altogether, the results indicated that S100A7 promotes osteoclast differentiation and function.

The requirement of M-CSF and RANKL in S100A7 enhanced osteoclast differentiation

Osteoclast precursors were differentiated in the presence or absence of M-SCF, RANKL and S100A7 (100ng/ml) to further investigate whether the stimulatory effect of S100A7 on osteoclast differentiation is dependent or independent of M-CSF and RANKL.

The results showed that without either M-CSF or RANKL, the differentiation of osteoclasts was compromised (Figure 35A). Addition of rhS100A7 did not increase the number of osteoclast in absence of either M-CSF or RANKL (Figure 35B). The results indicated that the stimulatory effect of S100A7 on osteoclast differentiation required both M-CSF and RANKL.

Expression of *RAGE* during S100A7 stimulated osteoclast differentiation

The expression of putative receptor of S100A7, *RAGE*, was determined in S100A7 induced osteoclast differentiation. Osteoclasts were differentiated in the presence or absence of rhS100A7 (100ng/ml). *RAGE* mRNA expression was determined at 4 and 7 days of differentiation. The results showed that *RAGE* expression was decreased during osteoclast differentiation. In the presence of rhS100A7, *RAGE* mRNA expression was significantly up-regulated at both day 4 and day 7 (Figure 36). However, decreasing pattern of *RAGE* expression during osteoclast differentiation was still observed. S100A7 induced *RAGE* expression in early and late osteoclast differentiation.

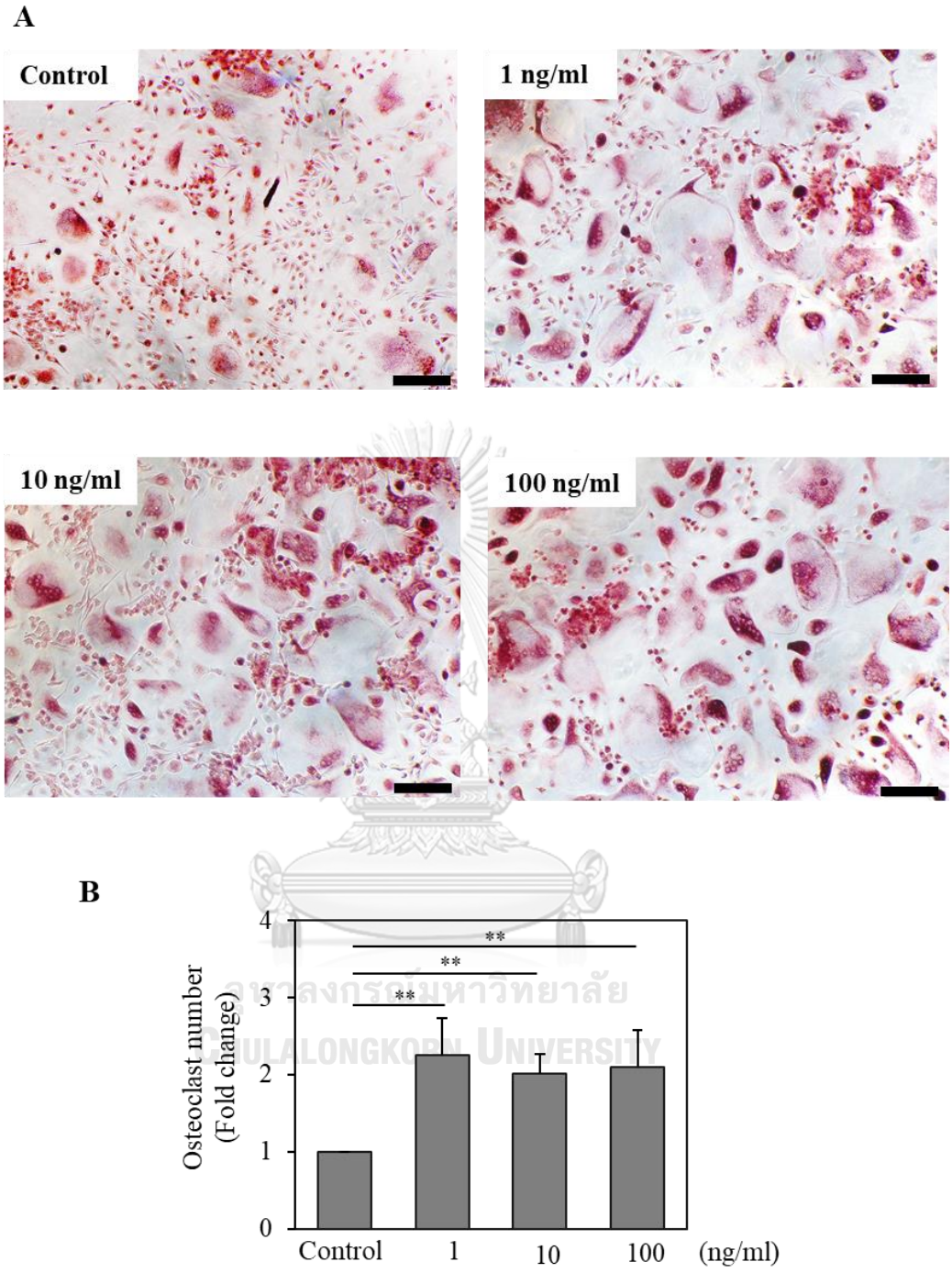

Figure 33 The increase in osteoclast number in the presence of rhS100A7. (**A**) Representative images of TRAP staining of osteoclasts cultured in the presence of various concentration of rhS100A7 and control cultured without rhS100A7 at 14 days of differentiation. (**B**) The number of osteoclasts was determined and compared to control. Value are presented as mean ± standard deviation (n=4), **p<0.01

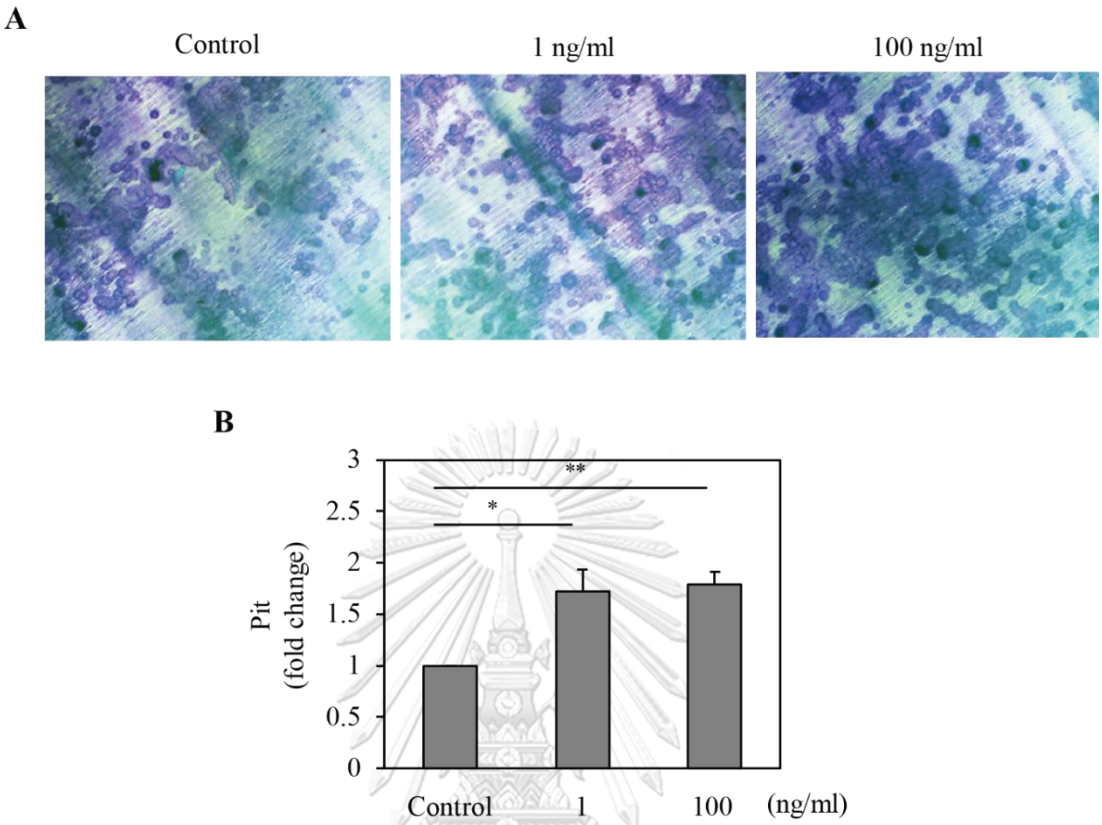

Figure 34 The increase in resorption pits formed by osteoclasts differentiated in the presence of rhS100A7. (**A**) Representative images of resorption pits in osteoclasts culture without rhS100A7 (control) and with S100A7 of 1 ng/ml and 100 ng/ml respectively. (**B**) The area of resorption pit was determined and compared to control. Value are presented as mean ± standard deviation (n=3), *p<0.05, **p<0.01

Expression of *RANK* during S100A7 stimulated osteoclast differentiation

The expression of *RANK* was also investigated in osteoclasts differentiated in the presence or absence of rhS100A7 (100ng/ml) at 4 and 7 days of differentiation. There was no difference in expression of *RANK* mRNA in both 4 days and 7 days of osteoclast differentiation in the presence of S100A7 (Figure 37) indicating that S100A7 did not affect *RANK* expression during osteoclast differentiation

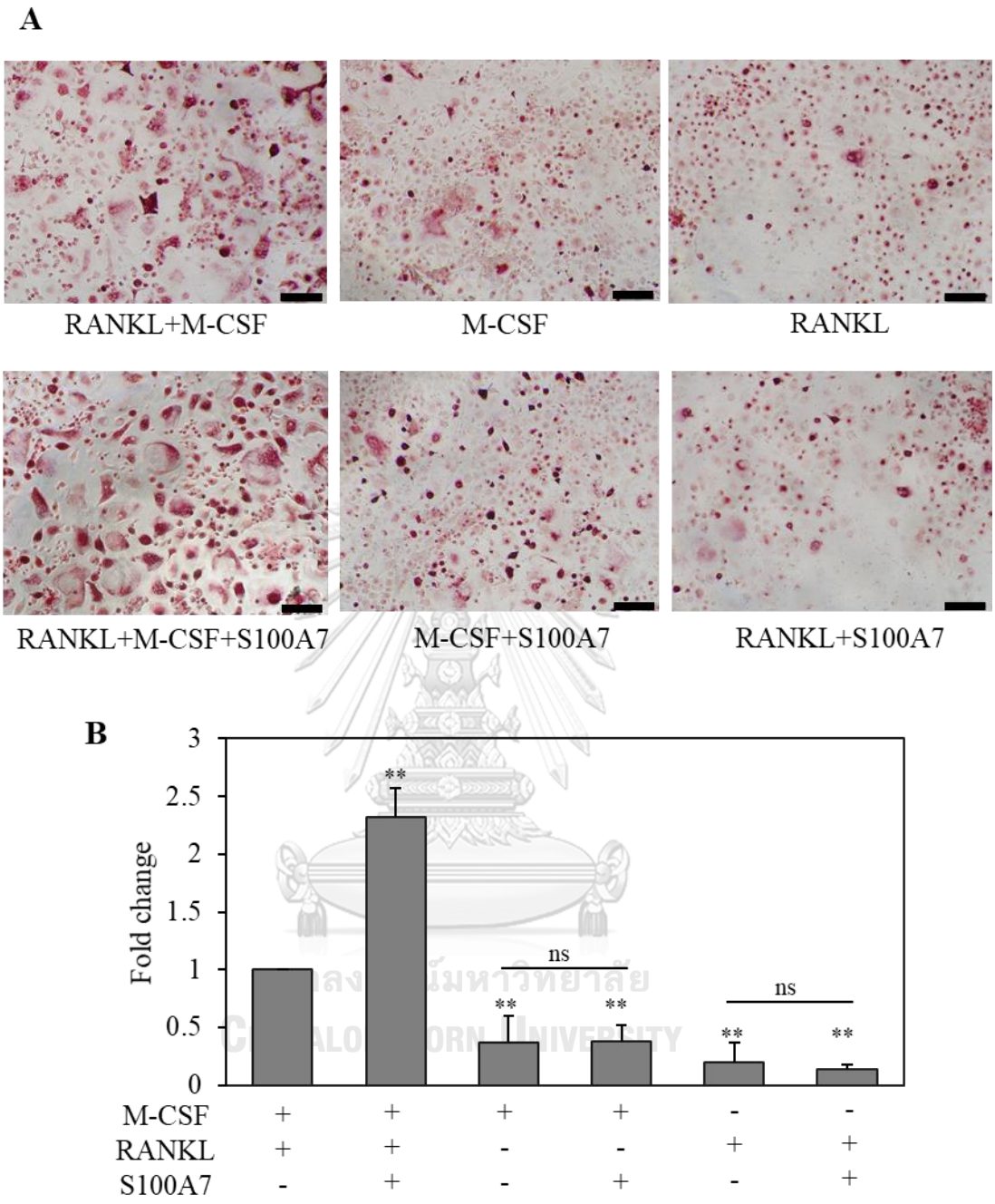

Figure 35 The number of osteoclasts differentiated in the absence or presence of rhS100A7 (100 ng/ml), rhM-CSF, and rhRANKL. Value are presented as mean ± standard deviation (n=4), **p<0.01 compared to control, ns=not significant.

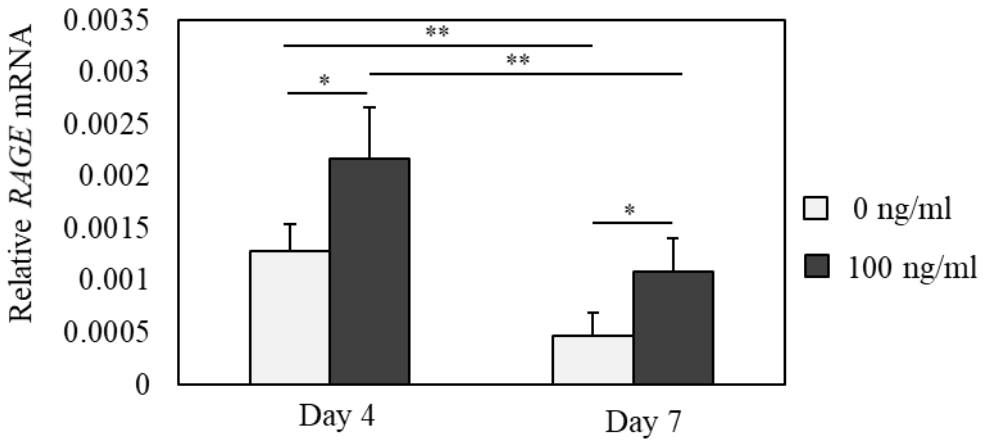

Figure 36 RAGE mRNA expression during osteoclast differentiation in 0 ng/ml (control) and 100 ng/ml rhS100A7. Value are presented as mean ± standard deviation (n=4). *p<0.05, **p<0.01

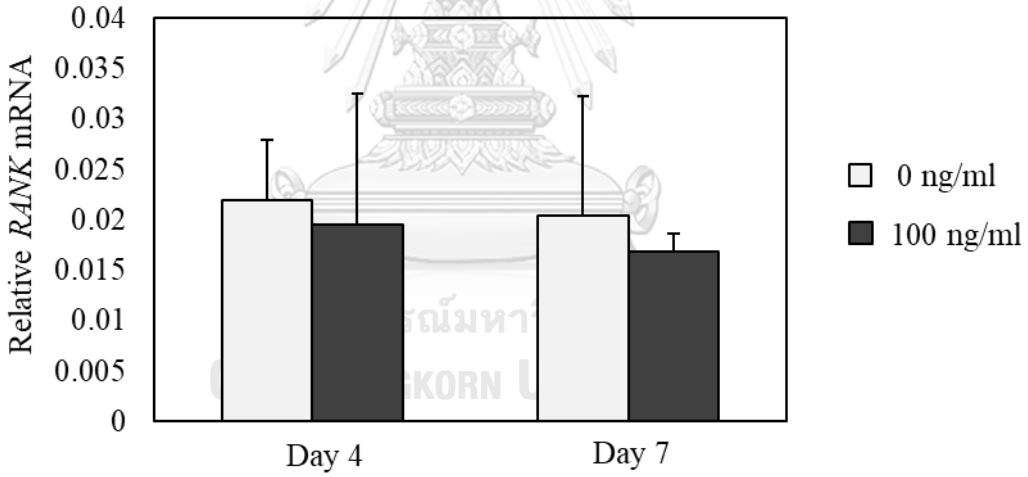

Figure 37 RANK mRNA expression during osteoclast differentiation in 0 ng/ml (control) and 100 ng/ml rhS100A7. Value are presented as mean ± standard deviation (n=4).

Chapter 5

Discussion

The in vitro force application model used in this study was the attempt to mimic the situation in which dental pulp cells were subjected to mechanical force that can cause pulpal inflammation. The results confirmed that the *in vitro* mechanical force application model used in this study did not cause cell death but can trigger inflammatory response as shown by the increase in expression of inflammatory cytokines, *IL1B*, *IL6* and *VEGF* (Figure 26). The increase expression of *IL6* following mechanical force application was also reported in previous studies in hDPCs [34] and SHED [35] using the same model of force application. In addition, Lee *et al* [37] found the increase in *IL1*, *TNFA*, and *IL6* gene expression in dental pulp cells subjected to mechanical strain. Up-regulation of *IL6* and *IL8* genes was also observed in PDL cells subjected to hydrostatic pressure as early as 10 minutes [33].

S100A7 is expressed mainly in epithelial component of the tissues. However, the results from this study showed that S100A7 are also expressed in hDPCs *in vitro* and dental pulp *in vivo* (Figure 27 and 29). In addition, there was the significant up-regulation of *S100A7* mRNA and S100A7 protein expression in hDPCs in response to mechanical force (Figure 27 and 30). In addition, the expression of *S100A7* in response to mechanical forced seemed to be specific to hDPCs since *S100A7* mRNA expression in hPDLs showed no significantly changes following mechanical stimulation (Figure 28). Moreover, compared to other *S100* investigated, *S100A7* was the only S100 upregulated in hDPCs in response to mechanical stress (Figure 27).

S100A4 which was previously found highly expressed in dental pulp cells [100] did not showed significantly changes in hDPCs following mechanical stress application (Figure 27). In addition, *S100A4* mRNA expression in hPDLs was significantly decreased when applying high force for long duration (2 g/cm^2 for 6h) (Figure 28). This result was in contrast to the finding of Duarte *et al* [101] that found upregulation of S100A4 in response to cyclical mechanical strain in bovine PDL cells. The different in S100A4 results in hDPLs, may due to the use of human and bovine PDLs. The type of

the force given was also different, in that, the continuous compressive force was used in this study while in study of Duarte *et al* [101], the cyclical stretching force was applied to the cells.

The changes in expression of *S100A8* gene, a well-known DAMPs [102, 103], following mechanical force application to hDPCs was highly varied so that no statistically significantly difference was observed (Figure 27). In contrast, in hPDLs, *S100A8* mRNA expression was significantly up-regulated in response to mechanical stress (Figure 28). This also confirmed the different response of hPDCs and hPDL to mechanical stress and that S100A7 was one of the molecules specifically up-regulated in response to mechanical stress of hDPCs.

To confirm the expression of *S100A7* in human dental pulp in response to mechanical stress *in vivo*, the orthodontic treatment was selected as the representative model of mechanical stress. Orthodontic force can be considered as one type of trauma and, as a result, pulp tissue can also be injured during orthodontic tooth movement. Orthodontic force was found to increase expression of inflammatory cytokines in dental pulp [104]. Transient pulpal inflammation, vascular changes, increase in fibrosis and pulp calcification was also observed following orthodontic treatment [36, 37, 105, 106]. Orthodontic tooth movement also cause an increase in RANKL in dental pulp of rats [104]. Moreover, it is well-known that orthodontic tooth movement increases the risk of root resorption [105, 107-109]. Therefore, in this study, orthodontic treatment was selected as the model of mechanical stress. The expression of *S100A7* in dental pulp of orthodontically moved teeth was compared to control teeth not subjected to orthodontic force. The significant higher level of *S100A7* mRNA in pulp tissue of orthodontically moved teeth compared to control, confirming the in vitro results that *S100A7* was up-regulated in human dental pulp in response to mechanical stress.

The possible mechanisms underlying mechanical stress-induced S100A7 in hDPCs may include the activation of P2X7R, EGF/EGFR and notch signaling. It has been reported that mechanical loading is sensed by the mechanosensitive P2X7 receptor (P2X7R), which is expressed in many cell types, including PDLs and hDPCs [110-112]. The activation of P2X7R by mechanical loading upregulated IL1β- and IL-6 expression [110, 111], which is concordant with the increased level of these two genes in hDPCs subjected to mechanical stress model in this study. In addition, evidences showed that

the activation of P2X7R also enhanced S100A7 expression [18]. Therefore, the increased *S100A7* mRNA expression and S100A7 protein production in hDPCs in response to mechanical loading may be via the activation of P2X7R.

EGF/EGFR signaling has been reported by many previous studies to be involved in activation of S100A7. In psoriasis, there is the increase in the number of EGFR and EGFR activation [18]. In ER-negative breast cancers, there was a high S100A7 and EGFR expression, and the correlation of S100A7 and EGFR was also observed [64]. Inhibition of EGFR resulted in marked inhibition of S100A7 expression following oncostatin-M treatment [21]. The association between S100A7 and an increase in EGF mRNA levels was observed in the study of Emberly *et al* [58]. Paruchuri *et al* [25] also found that EGF can increase the expression of S100A7 in MCF-7 and MDA-MB-468 cells in dose-dependent manner with the peak effect found at 70–100 ng/ml of EGF. In this study, although expression of EGFR was unchanged, there was the significant increase in *EGF* mRNA expression following 2 hours of mechanical force application (Figure 31), corresponding to the increase in *S100A7* mRNA expression (Figure 27). Thus, it is possible that S100A7 induction following mechanical loading was regulated through EGF. To further investigate the involvement of EGF/EGFR in S100A7 induction following mechanical stress, down-regulation of EGF and/or blocking of EGFR should be performed.

Higher expression of Notch and its ligands was observed in psoriatic skins, the disease with high expression of S100A7, compared to normal skin [113, 114]. The intensity of nuclear form of Notch 1 was also found associated with severity of psoriasis [113]. Moreover, many previous studies showed the relationship between Notch and dental pulp injuries [115]. Ma *et al* [116] found positive staining of Notch 2 after early days of mechanical injuries to dental pulp *in vivo* and was declined after 14 days. Notch 1 expression was found significantly increase in human deciduous dental pulp cells after applying static mechanical force [99]. Lovschall *et al* [117], found upregulation of *Notch* genes 1 day after pulp capping in rats which was decreased on day 3. A low increase in expression of notch ligands Delta-1 and Jagged-1 was also observed in the study of Lovschall *et al* [117] as well as the increase in notch target gene, Hes1. These indicated that notch signaling was activated in dental pulp in response to injury. In this study, although notch receptors genes were not up-regulated in response to mechanical

stress, the target genes, *HES1* mRNA was found significantly up-regulated (Figure 32) indicating that there may be an activation of notch signaling in hDPCs subjected to mechanical stress. However, further investigation of notch ligands and the down-stream signaling would help confirming the results. In addition, to investigate the relationship between S100A7 and notch signaling in hDPCs subjected to mechanical stress, further investigation is needed. This may include blocking of notch signaling by γ-secretase inhibitor and investigating S100A7 expression in response to mechanical stress of hDPCs.

S100A7 was found to secreted form hDPCs subjected to mechanical stress (Figure 30). Secreted S100A7 can have a chemotactic activity that induces the migration of lymphocytes, granulocytes and monocytes. S100A7 is also functions as a cytokine that activate the immune cells. S100A7 can induce many inflammatory cytokines including IL-6 and VEGF which resulted in promoting angiogenesis [23, 59, 63]. This correspond to the results from this study that *IL6* and *VEGF* was significantly up-regulated following mechanical force application and an up-regulation of S100A7 (Figure 31). The increase expression and secretion of S100A7 in the tissues, thus, may lead to the exacerbated inflammation [18, 24].

Several studies have illustrated that osteoclasts/odontoclasts are observed in the resorption area regardless of resorption types [2, 118, 119]. During inflammation, the immune cells and other local cells release chemokines and proinflammatory cytokines to recruit the precursor cells such as monocytes and macrophages [120, 121], and induce osteoclast/odontoclast differentiation [68, 122, 123]. Odontoclast is an osteoclast-like cell but it is located in the dental pulp and periodontal tissues [124]. The characteristics of odontoclasts are similar to those of osteoclasts i.e. the expression of cathepsin K, tartrate-resistant acid phosphatase (TRAP), H^+-ATPase and MMP-9 [124, 125] and the formation of clear zone and ruffled border [125]. In addition, it was suggested that, the resorption of bone and teeth shares common regulatory mechanisms [126]. Therefore, this study determined osteoclast differentiation and function by using peripheral blood monocyte as a precursor cells to represent the cells responding for root resorption.

The implication of S100A7 on osteoclast was reported in the study of Paruchuri *et al* [25] in murine cells in which S100A7 down-regulated breast cancer cells had the

decrease in ability to induce TRAP-positive cells formation and bone destruction. However, the direct effect of S100A7 on osteoclasts has not been investigated. In this study, there was the attempted to use the proteins directly produced from hDPCs to stimulate osteoclasts by using supernatant from control and mechanical stress-induced hDPCs to culture osteoclast precursors. However, supernatant from control hDPCs as well as stressed hDPCs seemed to affect viability of osteoclast precursors (data not shown). Therefore, the rhS100A7 with concentration found produced by hDPCs under mechanical stress was used to determine the direct effect of S100A7 on human osteoclast.

There was a significance increase in the number of osteoclasts as well as area of resorption in the presence of S100A7 from as low as 1 ng/ml (Figure 33 and 34) which correspond to the mean concentration of S100A7 found released from hDPCs subjected to mechanical force at 6 hours. Compared to other S100 proteins that have been reported to stimulate osteoclasts, the stimulating effect of S100A7 on osteoclasts seem to be more potent. The results from this study found as little as 1 ng/ml of S100A7 can significantly increase osteoclast number and area of resorption to approximately 2 folds. Grevers *et al* [94] found 1.5- and 2-fold increase in percentage of bone resorption when treated with recombinant S100A8 at 1 and 5 ug/ml respectively but with lower concentration of S100A8 at 200 ng, no significant changes in percentage of bone resorption was observed. Mah *et al* [91] found that recombinant S100A4 of 1 ug/ml can increase the number of osteoclast to approximately 2 folds.

Osteoclast differentiation required the signal from RANKL and M-CSF [68]. Without either M-CSF and RANKL, the differentiation of osteoclast was compromised as found in this study (Figure 35). Nicholson *et al* [127] also showed the reduction in $TRAP^+$ multinuclear cells when $CD14^+$ cells were culture in M-CSF alone compared to when cultured with both M-CSF and RANKL which is correspond to the results in this study.

Many biological molecules have been reported to promoted osteoclast. Some of these molecules were reported to stimulate osteoclast differentiation independent of RANKL, while others were found to have RANKL-dependent stimulatory effect on osteoclasts [85, 128, 129]. In this study, we found that S100A7 could not substitute to

either M-CSF or RANKL but it could produce additional stimulatory effect on osteoclast differentiation only in the presence of both M-CSF and RANKL (Figure 35).

Since S100A7 stimulate osteoclast differentiation dependent on RANKL, it was hypothesized that S100A7 may stimulate osteoclastogenesis by increasing RANK expression. Regulation of osteoclast through regulation of RANK expression has been shown for IL-4 and IL-13. These two cytokines down-regulated RANK and suppress RANKL-induced osteoclastogenesis and bone resorption [130]. Acetylcholinesterase was found to stimulate osteoclast differentiation possibly through mediating RANK expression. Acetylcholinesterase stimulated RANKL-induced osteoclast differentiation with an increase in RANK. Blocking of acetylcholinesterase using Donepezil can decrease RANK expression in bone marrow macrophages resulting in down-regulation of c-Fos and suppression osteoclast differentiation [131].

Evidences have revealed that RAGE is a putative receptor of S100A7 [24]. RAGE is expressed in monocytes and macrophages, which can differentiate to osteoclasts [121]. RAGE and its ligands was reported to be able to stimulate osteoclastic activity [89]. The expression of RAGE is induced by RANKL [84], and is upregulated upon osteoclast differentiation [84, 89, 90]. $RAGE^{-/-}$ mice exhibited the increased bone mass due to the impaired osteoclast formation and function [84]. RAGE was reported to involve in RANKL-induced and integrin-dependent osteoclastogenesis [132]. Furthermore, $RAGE^{-/-}$ osteoclastic precursors failed to respond to M-CSF and RANKL [84, 89].

In this study, the results showed that RAGE was expressed during osteoclast differentiation and it was significantly upregulated in the presence of rhS100A7 in both early and later period of differentiations while expression of RANK, one of the receptors providing main signaling in osteoclast differentiation, was not affected by S100A7 (Figure 36 and 37).

RAGE may mediate osteoclast differentiation by regulation of integrin signaling which can have the functional crosstalk with M-CSF and RANKL pathway in activation of osteoclasts [82]. Integrin αvβ3 was found to associated activated RANK in the presence of c-Src which bind to SH2 domain of RANK and SH3 domain of αvβ3 [82, 83]. This collaboration of activated RANK and αvβ3 pathway stimulate the

canonical pathway that include activation of c-Src, Syk, Slp76, Vav3 and Rac resulting in cytoskeletal organization [83].

RAGE may regulate integrin via direct binding or regulation at transcriptional level [84]. During osteoclast differentiation, there was the up-regulation of αvβ3 in wild-type osteoclast, while delayed and reduced in the induction of αvβ3 was observed in $RAGE^{-/-}$ bone marrow macrophages [84]. RAGE was also reported to have a role in sustained ERK activation which is essential for expression of integrin β3 [84]. Integrin β3 was highly expressed in mature osteoclast while monocytes and osteoclast precursors expressed β2 integrins [133]. β2 integrins can suppress osteoclast differentiation in early phase by preventing induction of NFATc1. RANKL has been found to induce the switch from β2 to β3 integrins. This down-regulation of β2 integrin by RANKL suppress the negative regulator of osteoclast differentiation, thus, promoting osteoclast differentiation.

RAGE mediated osteoclastogenesis may also involve in activation integrin convergent downstream signal including PYK2, Src, Rac, and Erk which further activate the C-Fos, AP-1 and NFATc1, the transcriptional factors essential for osteoclast differentiation [84]. Impairing of αvβ3 integrin signaling was also observed in $RAGE^{-/-}$ bone marrow macrophages and osteoclast precursors [84]. Furthermore, RAGE may have a role in linking c-FMS to produce these integrin convergent downstream signals [84] (Figure 38).

Therefore, it is possible that S100A7 regulated expression of RAGE may regulate integrin signaling resulting in promoting RANKL and M-CSF induced osteoclast differentiation which was observed in this study. However, further investigation is needed, for example, blocking of RAGE to confirm the involvement this receptor in S100A7 stimulated osteoclastogenesis. In addition, since previous study found that S100A8 can mediate osteoclast differentiation through TLR4 but not RAGE [94]. Therefore, further investigation of other S100A7 putative receptors would further clarify the mechanisms underlying S100A7 mediated osteoclastogenesis.

Apart from S100A7, many other factors presented in inflamed dental pulp following mechanical injuries may also play a role in stimulation of osteoclast differentiation. Previous study found that orthodontic force increased RANKL in dental pulp which may regulated by an increase in IL-17 [104]. IL-6 that found up-regulated

in dental pulp following mechanical stress in this study and many previous study, can also activate osteoclast in RANK/RANKL-independent pathway [85]. The non-canonical pathways of osteoclast differentiation, which is the stimulation of osteoclastogenesis by other factors apart from RANKL, are believed to play a role in pathologic bone resorption [69, 73]. These molecules may act together with S100A7 in activation of osteoclasts following mechanical stress in dental pulp.

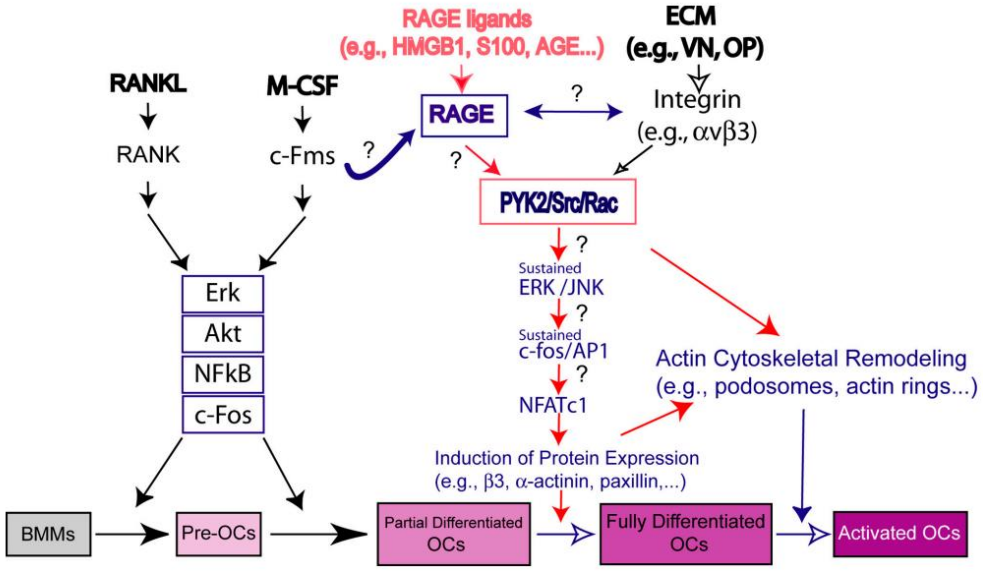

Figure 38 The possible mechanisms involving RAGE in osteoclast differentiation (Picture from Zhou et al [84])

In conclusion, this study found that following mechanical stress application, S100A7 was induced in dental pulp, which has the effect to stimulate osteoclastogenesis. This study provides the increase in the knowledge of the molecules underlying mechanical stressed-induced human dental pulp that potentially enhance RANKL and M-CFS stimulated osteoclast differentiation (Figure 39).

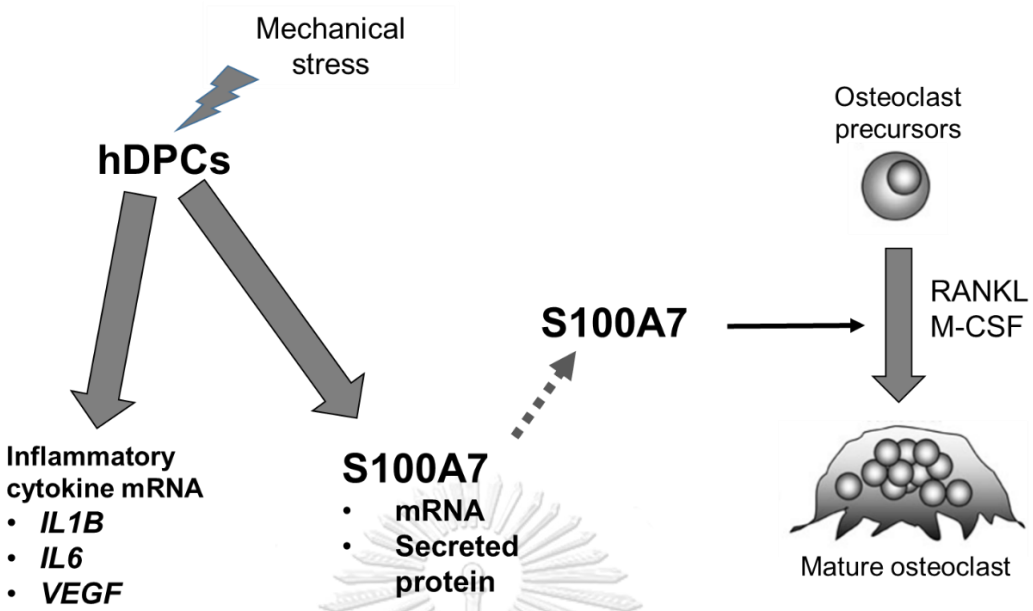

Figure 39 Summary of the findings from this study. Following mechanical stress, human dental pulp cells up-regulate inflammatory cytokine IL1B, IL6 and VEGF mRNA. Increase in S100A7 was also observed in both transcript and secreted protein level. S100A7 has the stimulatory effect in RANKL- and M-CSF-induced osteoclast differentiation.

REFERENCES

1. Fernandes, M., I. de Ataide, and R. Wagle, *Tooth resorption part I - pathogenesis and case series of internal resorption.* J Conserv Dent, 2013. **16**(1): p. 4-8.
2. Patel, S., et al., *Internal root resorption: a review.* J Endod, 2010. **36**(7): p. 1107-21.
3. Thomas, P., et al., *An insight into internal resorption.* ISRN Dent, 2014. **2014**: p. 759326.
4. Tyrovola, J.B., et al., *Root resorption and the OPG/RANKL/RANK system: a mini review.* J Oral Sci, 2008. **50**(4): p. 367-76.
5. Gabor, C., et al., *Prevalence of internal inflammatory root resorption.* J Endod, 2012. **38**(1): p. 24-7.
6. Consolaro, A. and L.Z. Furquim, *Extreme root resorption associated with induced tooth movement: a protocol for clinical management.* Dental Press J Orthod, 2014. **19**(5): p. 19-26.
7. Soares, A.J., et al., *Frequency of root resorption following trauma to permanent teeth.* J Oral Sci, 2015. **57**(2): p. 73-8.
8. Bastos, J.V., et al., *Age and timing of pulp extirpation as major factors associated with inflammatory root resorption in replanted permanent teeth.* J Endod, 2014. **40**(3): p. 366-71.
9. Mattison, G.D., L.R. Gholston, and P. Boyd, *Orthodontic external root resorption--endodontic considerations.* J Endod, 1983. **9**(6): p. 253-6.
10. Mincik, J., D. Urban, and S. Timkova, *Clinical Management of Two Root Resorption Cases in Endodontic Practice.* Case Rep Dent, 2016. **2016**: p. 9075363.
11. Bender, I.B., M.R. Byers, and K. Mori, *Periapical replacement resorption of permanent, vital, endodontically treated incisors after orthodontic movement: report of two cases.* J Endod, 1997. **23**(12): p. 768-73.
12. Kaku, M., et al., *Effects of pulpectomy on the amount of root resorption during orthodontic tooth movement.* J Endod, 2014. **40**(3): p. 372-8.

13. Lee, Y.J. and T.Y. Lee, *External root resorption during orthodontic treatment in root-filled teeth and contralateral teeth with vital pulp: A clinical study of contributing factors.* Am J Orthod Dentofacial Orthop, 2016. **149**(1): p. 84-91.
14. Mjor, I.A. and K. Heyeraas, *Pulp-dentin and periodontal anatomy and physiology*, in *Essential Endodontology*, D. Orstavik and T.P. Ford, Editors. 2008, Blackwell Munksgaard Ltd.
15. Heyeraas, K.J. and E. Berggreen, *Interstitial fluid pressure in normal and inflamed pulp.* Crit Rev Oral Biol Med, 1999. **10**(3): p. 328-36.
16. Madsen, P., et al., *Molecular cloning, occurrence, and expression of a novel partially secreted protein "psoriasin" that is highly up-regulated in psoriatic skin.* J Invest Dermatol, 1991. **97**(4): p. 701-12.
17. Glaser, R., et al., *The antimicrobial protein psoriasin (S100A7) is upregulated in atopic dermatitis and after experimental skin barrier disruption.* J Invest Dermatol, 2009. **129**(3): p. 641-9.
18. D'Amico, F., et al., *S100A7: A rAMPing up AMP molecule in psoriasis.* Cytokine Growth Factor Rev, 2016. **32**: p. 97-104.
19. Gazel, A., et al., *A characteristic subset of psoriasis-associated genes is induced by oncostatin-M in reconstituted epidermis.* J Invest Dermatol, 2006. **126**(12): p. 2647-57.
20. Liang, S.C., et al., *Interleukin (IL)-22 and IL-17 are coexpressed by Th17 cells and cooperatively enhance expression of antimicrobial peptides.* J Exp Med, 2006. **203**(10): p. 2271-9.
21. West, N.R. and P.H. Watson, *S100A7 (psoriasin) is induced by the proinflammatory cytokines oncostatin-M and interleukin-6 in human breast cancer.* Oncogene, 2010. **29**(14): p. 2083-92.
22. Batycka-Baran, A., et al., *Leukocyte-derived koebnerisin (S100A15) and psoriasin (S100A7) are systemic mediators of inflammation in psoriasis.* J Dermatol Sci, 2015. **79**(3): p. 214-21.
23. Nasser, M.W., et al., *S100A7 enhances mammary tumorigenesis through upregulation of inflammatory pathways.* Cancer Res, 2012. **72**(3): p. 604-15.
24. Wolf, R., et al., *Chemotactic activity of S100A7 (Psoriasin) is mediated by the receptor for advanced glycation end products and potentiates inflammation with*

highly homologous but functionally distinct S100A15. J Immunol, 2008. **181**(2): p. 1499-506.

25. Paruchuri, V., et al., *S100A7-downregulation inhibits epidermal growth factor-induced signaling in breast cancer cells and blocks osteoclast formation.* PLoS One, 2008. **3**(3): p. e1741.
26. Dabas, U. and V. Dabas, *Textbook of Endodontics*. 1st ed. 2007: AITBS publisher.
27. Arana-Chavez, V.E. and L.F. Massa, *Odontoblasts: the cells forming and maintaining dentine.* Int J Biochem Cell Biol, 2004. **36**(8): p. 1367-73.
28. Kawashima, N. and T. Okiji, *Odontoblasts: Specialized hard-tissue-forming cells in the dentin-pulp complex.* Congenit Anom (Kyoto), 2016. **56**(4): p. 144-53.
29. Gronthos, S., et al., *Postnatal human dental pulp stem cells (DPSCs) in vitro and in vivo.* Proc Natl Acad Sci U S A, 2000. **97**(25): p. 13625-30.
30. Gronthos, S., et al., *Stem cell properties of human dental pulp stem cells.* J Dent Res, 2002. **81**(8): p. 531-5.
31. Shekar, R. and K. Ranganathan, *Phenotypic and growth characterization of human mesenchymal stem cells cultured from permanent and deciduous teeth.* Indian J Dent Res, 2012. **23**(6): p. 838-9.
32. Levy Nogueira, M., et al., *Mechanical Stress as the Common Denominator between Chronic Inflammation, Cancer, and Alzheimer's Disease.* Front Oncol, 2015. **5**: p. 197.
33. Yamamoto, T., et al., *Mechanical stress induces expression of cytokines in human periodontal ligament cells.* Oral Dis, 2006. **12**(2): p. 171-5.
34. Satrawaha, S., et al., *Pressure induces interleukin-6 expression via the P2Y6 receptor in human dental pulp cells.* Arch Oral Biol, 2011. **56**(11): p. 1230-7.
35. Govitvattana, N., et al., *IL-6 regulated stress-induced Rex-1 expression in stem cells from human exfoliated deciduous teeth.* Oral Dis, 2013. **19**(7): p. 673-82.
36. Bletsa, A., E. Berggreen, and P. Brudvik, *Interleukin-1alpha and tumor necrosis factor-alpha expression during the early phases of orthodontic tooth movement in rats.* Eur J Oral Sci, 2006. **114**(5): p. 423-9.
37. Lee, S.K., et al., *Mechanical stress activates proinflammatory cytokines and antioxidant defense enzymes in human dental pulp cells.* J Endod, 2008. **34**(11): p. 1364-9.

38. Yu, V., et al., *Dynamic hydrostatic pressure promotes differentiation of human dental pulp stem cells.* Biochem Biophys Res Commun, 2009. **386**(4): p. 661-5.
39. Lee, S.K., et al., *Mechanical stress promotes odontoblastic differentiation via the heme oxygenase-1 pathway in human dental pulp cell line.* Life Sci, 2010. **86**(3-4): p. 107-14.
40. Caviedes-Bucheli, J., et al., *The effect of orthodontic forces on calcitonin gene-related peptide expression in human dental pulp.* J Endod, 2011. **37**(7): p. 934-7.
41. Sedaghat, F. and A. Notopoulos, *S100 protein family and its application in clinical practice.* Hippokratia, 2008. **12**(4): p. 198-204.
42. Marenholz, I., C.W. Heizmann, and G. Fritz, *S100 proteins in mouse and man: from evolution to function and pathology (including an update of the nomenclature).* Biochem Biophys Res Commun, 2004. **322**(4): p. 1111-22.
43. Donato, R., et al., *Functions of S100 proteins.* Curr Mol Med, 2013. **13**(1): p. 24-57.
44. Srikrishna, G. and H.H. Freeze, *S100 protein family and tumorigenesis.* Atlas Genet Cytogenet Oncol Haematol, 2011. **15**(9): p. 768-776.
45. Chen, H., et al., *S100 protein family in human cancer.* Am J Cancer Res, 2014. **4**(2): p. 89-115.
46. Salama, I., et al., *A review of the S100 proteins in cancer.* Eur J Surg Oncol, 2008. **34**(4): p. 357-64.
47. Bresnick, A.R., D.J. Weber, and D.B. Zimmer, *S100 proteins in cancer.* Nat Rev Cancer, 2015. **15**(2): p. 96-109.
48. Fuentes, M.K., et al., *RAGE activation by S100P in colon cancer stimulates growth, migration, and cell signaling pathways.* Dis Colon Rectum, 2007. **50**(8): p. 1230-40.
49. Watson, P.H., E.R. Leygue, and L.C. Murphy, *Psoriasin (S100A7).* Int J Biochem Cell Biol, 1998. **30**(5): p. 567-71.
50. Semprini, S., et al., *Genomic structure, promoter characterisation and mutational analysis of the S100A7 gene: exclusion of a candidate for familial psoriasis susceptibility.* Hum Genet, 1999. **104**(2): p. 130-4.
51. Leclerc, E., et al., *Binding of S100 proteins to RAGE: an update.* Biochim Biophys Acta, 2009. **1793**(6): p. 993-1007.

52. Rangaraj, A., et al., *Molecular and cellular impact of Psoriasin (S100A7) on the healing of human wounds.* Exp Ther Med, 2017. **13**(5): p. 2151-2160.
53. Ruse, M., A.M. Broome, and R.L. Eckert, *S100A7 (psoriasin) interacts with epidermal fatty acid binding protein and localizes in focal adhesion-like structures in cultured keratinocytes.* J Invest Dermatol, 2003. **121**(1): p. 132-41.
54. Al-Haddad, S., et al., *Psoriasin (S100A7) expression and invasive breast cancer.* Am J Pathol, 1999. **155**(6): p. 2057-66.
55. Enerback, C., et al., *Psoriasin expression in mammary epithelial cells in vitro and in vivo.* Cancer Res, 2002. **62**(1): p. 43-7.
56. Deol, Y.S., et al., *Tumor-suppressive effects of psoriasin (S100A7) are mediated through the beta-catenin/T cell factor 4 protein pathway in estrogen receptor-positive breast cancer cells.* J Biol Chem, 2011. **286**(52): p. 44845-54.
57. Emberley, E.D., et al., *Psoriasin (S100A7) expression is associated with poor outcome in estrogen receptor-negative invasive breast cancer.* Clin Cancer Res, 2003. **9**(7): p. 2627-31.
58. Emberley, E.D., et al., *The S100A7-c-Jun activation domain binding protein 1 pathway enhances prosurvival pathways in breast cancer.* Cancer Res, 2005. **65**(13): p. 5696-702.
59. Krop, I., et al., *A putative role for psoriasin in breast tumor progression.* Cancer Res, 2005. **65**(24): p. 11326-34.
60. Kataoka, K., et al., *S100A7 promotes the migration and invasion of osteosarcoma cells via the receptor for advanced glycation end products.* Oncol Lett, 2012. **3**(5): p. 1149-1153.
61. Padilla, L., et al., *S100A7: from mechanism to cancer therapy.* Oncogene, 2017. **36**(49): p. 6749-6761.
62. Boniface, K., et al., *IL-22 inhibits epidermal differentiation and induces proinflammatory gene expression and migration of human keratinocytes.* J Immunol, 2005. **174**(6): p. 3695-702.
63. Zheng, Y., et al., *Microbicidal protein psoriasin is a multifunctional modulator of neutrophil activation.* Immunology, 2008. **124**(3): p. 357-67.
64. Wang, J., et al., *Jab1 is a target of EGFR signaling in ERalpha-negative breast cancer.* Breast Cancer Res, 2008. **10**(3): p. R51.

65. Onderdijk, A.J., et al., *IL-4 Downregulates IL-1beta and IL-6 and Induces GATA3 in Psoriatic Epidermal Cells: Route of Action of a Th2 Cytokine.* J Immunol, 2015. **195**(4): p. 1744-52.
66. Teng, X., et al., *IL-37 ameliorates the inflammatory process in psoriasis by suppressing proinflammatory cytokine production.* J Immunol, 2014. **192**(4): p. 1815-23.
67. Blair, H.C. and N.A. Athanasou, *Recent advances in osteoclast biology and pathological bone resorption.* Histol Histopathol, 2004. **19**(1): p. 189-99.
68. Edwards, J.R. and G.R. Mundy, *Advances in osteoclast biology: old findings and new insights from mouse models.* Nat Rev Rheumatol, 2011. **7**(4): p. 235-43.
69. Sabokbar, A., et al., *Non-Canonical (RANKL-Independent) Pathways of Osteoclast Differentiation and Their Role in Musculoskeletal Diseases.* Clin Rev Allergy Immunol, 2016. **51**(1): p. 16-26.
70. Soysa, N.S., et al., *Osteoclast formation and differentiation: an overview.* J Med Dent Sci, 2012. **59**(3): p. 65-74.
71. Duong, L.T., et al., *Integrins and signaling in osteoclast function.* Matrix Biol, 2000. **19**(2): p. 97-105.
72. Boyle, W.J., W.S. Simonet, and D.L. Lacey, *Osteoclast differentiation and activation.* Nature, 2003. **423**(6937): p. 337-42.
73. Novack, D.V. and G. Mbalaviele, *Osteoclasts-Key Players in Skeletal Health and Disease.* Microbiol Spectr, 2016. **4**(3).
74. Takayanagi, H., *Osteoimmunology: shared mechanisms and crosstalk between the immune and bone systems.* Nat Rev Immunol, 2007. **7**(4): p. 292-304.
75. Negishi-Koga, T. and H. Takayanagi, *Ca2+-NFATc1 signaling is an essential axis of osteoclast differentiation.* Immunol Rev, 2009. **231**(1): p. 241-56.
76. Kim, J.H. and N. Kim, *Signaling Pathways in Osteoclast Differentiation.* Chonnam Med J, 2016. **52**(1): p. 12-7.
77. Takayanagi, H., *The role of NFAT in osteoclast formation.* Ann N Y Acad Sci, 2007. **1116**: p. 227-37.
78. Kim, J.H. and N. Kim, *Regulation of NFATc1 in Osteoclast Differentiation.* J Bone Metab, 2014. **21**(4): p. 233-41.

79. Wagner, E.F. and K. Matsuo, *Signalling in osteoclasts and the role of Fos/AP1 proteins.* Ann Rheum Dis, 2003. **62 Suppl 2**: p. ii83-5.
80. Kajiya, M., et al., *Role of periodontal pathogenic bacteria in RANKL-mediated bone destruction in periodontal disease.* J Oral Microbiol, 2010. **2**.
81. Asagiri, M. and H. Takayanagi, *The molecular understanding of osteoclast differentiation.* Bone, 2007. **40**(2): p. 251-64.
82. Feng, X. and S.L. Teitelbaum, *Osteoclasts: New Insights.* Bone Res, 2013. **1**(1): p. 11-26.
83. Izawa, T., et al., *c-Src links a RANK/alphavbeta3 integrin complex to the osteoclast cytoskeleton.* Mol Cell Biol, 2012. **32**(14): p. 2943-53.
84. Zhou, Z., et al., *Regulation of osteoclast function and bone mass by RAGE.* J Exp Med, 2006. **203**(4): p. 1067-80.
85. O'Brien, W., et al., *RANK-Independent Osteoclast Formation and Bone Erosion in Inflammatory Arthritis.* Arthritis Rheumatol, 2016. **68**(12): p. 2889-2900.
86. Knowles, H.J. and N.A. Athanasou, *Canonical and non-canonical pathways of osteoclast formation.* Histol Histopathol, 2009. **24**(3): p. 337-46.
87. Charles, J.F. and M.C. Nakamura, *Bone and the innate immune system.* Curr Osteoporos Rep, 2014. **12**(1): p. 1-8.
88. Bar-Shavit, Z., *Taking a toll on the bones: regulation of bone metabolism by innate immune regulators.* Autoimmunity, 2008. **41**(3): p. 195-203.
89. Zhou, Z. and W.C. Xiong, *RAGE and its ligands in bone metabolism.* Front Biosci (Schol Ed), 2011. **3**: p. 768-76.
90. Kosaka, T., et al., *RAGE, receptor of advanced glycation endoproducts, negatively regulates chondrocytes differentiation.* PLoS One, 2014. **9**(9): p. e108819.
91. Mah, S.J., et al., *Induction of S100A4 in periodontal ligament cells enhances osteoclast formation.* Arch Oral Biol, 2015. **60**(9): p. 1215-21.
92. Erlandsson, M.C., et al., *Expression of metastasin S100A4 is essential for bone resorption and regulates osteoclast function.* Biochim Biophys Acta, 2013. **1833**(12): p. 2653-63.
93. Zreiqat, H., et al., *S100A8/S100A9 and their association with cartilage and bone.* J Mol Histol, 2007. **38**(5): p. 381-91.

94. Grevers, L.C., et al., *S100A8 enhances osteoclastic bone resorption in vitro through activation of Toll-like receptor 4: implications for bone destruction in murine antigen-induced arthritis.* Arthritis Rheum, 2011. **63**(5): p. 1365-75.
95. La Noce, M., et al., *Dental pulp stem cells: state of the art and suggestions for a true translation of research into therapy.* J Dent, 2014. **42**(7): p. 761-8.
96. Kanzaki, H., et al., *Periodontal ligament cells under mechanical stress induce osteoclastogenesis by receptor activator of nuclear factor kappaB ligand up-regulation via prostaglandin E2 synthesis.* J Bone Miner Res, 2002. **17**(2): p. 210-20.
97. Wongkhantee, S., T. Yongchaitrakul, and P. Pavasant, *Mechanical stress induces osteopontin via ATP/P2Y1 in periodontal cells.* J Dent Res, 2008. **87**(6): p. 564-8.
98. Manokawinchoke, J., et al., *Mechanical Force-induced TGFB1 Increases Expression of SOST/POSTN by hPDL Cells.* J Dent Res, 2015. **94**(7): p. 983-9.
99. Peetiakarawach, K., et al., *Compressive Stress Enhances NOTCH1 mRNA Expression in Human Deciduous Dental Pulp Cells in vitro.* CU Dent J, 2015. **38**(Suppl): p. 13-20.
100. Duarte, W.R., et al., *cDNA cloning of S100 calcium-binding proteins from bovine periodontal ligament and their expression in oral tissues.* J Dent Res, 1998. **77**(9): p. 1694-9.
101. Duarte, W.R., et al., *Effects of mechanical stress on the mRNA expression of S100A4 and cytoskeletal components by periodontal ligament cells.* J Med Dent Sci, 1999. **46**(3): p. 117-22.
102. Bianchi, M.E., *DAMPs, PAMPs and alarmins: all we need to know about danger.* J Leukoc Biol, 2007. **81**(1): p. 1-5.
103. Rosin, D.L. and M.D. Okusa, *Dangers within: DAMP responses to damage and cell death in kidney disease.* J Am Soc Nephrol, 2011. **22**(3): p. 416-25.
104. Nakano, Y., et al., *Interleukin-17 is involved in orthodontically induced inflammatory root resorption in dental pulp cells.* Am J Orthod Dentofacial Orthop, 2015. **148**(2): p. 302-9.
105. Talic, N.F., *Adverse effects of orthodontic treatment: A clinical perspective.* Saudi Dent J, 2011. **23**(2): p. 55-9.

106. Lazzaretti, D.N., et al., *Histologic evaluation of human pulp tissue after orthodontic intrusion.* J Endod, 2014. **40**(10): p. 1537-40.
107. Jung, Y.H. and B.H. Cho, *External root resorption after orthodontic treatment: a study of contributing factors.* Imaging Sci Dent, 2011. **41**(1): p. 17-21.
108. Lund, H., et al., *Apical root resorption during orthodontic treatment. A prospective study using cone beam CT.* Angle Orthod, 2012. **82**(3): p. 480-7.
109. Topkara, A., A.I. Karaman, and C.H. Kau, *Apical root resorption caused by orthodontic forces: A brief review and a long-term observation.* Eur J Dent, 2012. **6**(4): p. 445-53.
110. Kanjanamekanant, K., P. Luckprom, and P. Pavasant, *Mechanical stress-induced interleukin-1beta expression through adenosine triphosphate/P2X7 receptor activation in human periodontal ligament cells.* J Periodontal Res, 2013. **48**(2): p. 169-76.
111. Lu, W., et al., *The P2X7 receptor links mechanical strain to cytokine IL-6 up-regulation and release in neurons and astrocytes.* J Neurochem, 2017. **141**(3): p. 436-448.
112. Wang, W., et al., *Effects of Adenosine Triphosphate on Proliferation and Odontoblastic Differentiation of Human Dental Pulp Cells.* J Endod, 2016. **42**(10): p. 1483-9.
113. Abdou, A.G., et al., *Up-regulation of Notch-1 in psoriasis: an immunohistochemical study.* Ann Diagn Pathol, 2012. **16**(3): p. 177-84.
114. Rooney, P., et al., *Notch-1 mediates endothelial cell activation and invasion in psoriasis.* Exp Dermatol, 2014. **23**(2): p. 113-8.
115. Mitsiadis, T.A., et al., *Monitoring Notch Signaling-Associated Activation of Stem Cell Niches within Injured Dental Pulp.* Front Physiol, 2017. **8**: p. 372.
116. Ma, L., et al., *Activation and dynamic expression of Notch signalling in dental pulp cells after injury in vitro and in vivo.* Int Endod J, 2016. **49**(12): p. 1165-1174.
117. Lovschall, H., et al., *Activation of the Notch signaling pathway in response to pulp capping of rat molars.* Eur J Oral Sci, 2005. **113**(4): p. 312-7.
118. Wedenberg, C. and S. Lindskog, *Experimental internal resorption in monkey teeth.* Endod Dent Traumatol, 1985. **1**(6): p. 221-7.

119. Wedenberg, C. and L. Zetterqvist, *Internal resorption in human teeth--a histological, scanning electron microscopic, and enzyme histochemical study.* J Endod, 1987. **13**(6): p. 255-9.
120. Rechenberg, D.K., J.C. Galicia, and O.A. Peters, *Biological Markers for Pulpal Inflammation: A Systematic Review.* PLoS One, 2016. **11**(11): p. e0167289.
121. Udagawa, N., et al., *Origin of osteoclasts: mature monocytes and macrophages are capable of differentiating into osteoclasts under a suitable microenvironment prepared by bone marrow-derived stromal cells.* Proc Natl Acad Sci U S A, 1990. **87**(18): p. 7260-4.
122. Silva, T.A., et al., *Chemokines in oral inflammatory diseases: apical periodontitis and periodontal disease.* J Dent Res, 2007. **86**(4): p. 306-19.
123. Takayanagi, H., *New immune connections in osteoclast formation.* Ann N Y Acad Sci, 2010. **1192**: p. 117-23.
124. Sahara, N., et al., *Cytodifferentiation of the odontoclast prior to the shedding of human deciduous teeth: an ultrastructural and cytochemical study.* Anat Rec, 1996. **244**(1): p. 33-49.
125. Wang, Z. and L.K. McCauley, *Osteoclasts and odontoclasts: signaling pathways to development and disease.* Oral Dis, 2011. **17**(2): p. 129-42.
126. Sasaki, T., *Differentiation and functions of osteoclasts and odontoclasts in mineralized tissue resorption.* Microsc Res Tech, 2003. **61**(6): p. 483-95.
127. Nicholson, G.C., et al., *Induction of osteoclasts from CD14-positive human peripheral blood mononuclear cells by receptor activator of nuclear factor kappaB ligand (RANKL).* Clin Sci (Lond), 2000. **99**(2): p. 133-40.
128. Dai, S.M., K. Nishioka, and K. Yudoh, *Interleukin (IL) 18 stimulates osteoclast formation through synovial T cells in rheumatoid arthritis: comparison with IL1 beta and tumour necrosis factor alpha.* Ann Rheum Dis, 2004. **63**(11): p. 1379-86.
129. Kudo, O., et al., *Interleukin-6 and interleukin-11 support human osteoclast formation by a RANKL-independent mechanism.* Bone, 2003. **32**(1): p. 1-7.
130. Palmqvist, P., et al., *Inhibition of hormone and cytokine-stimulated osteoclastogenesis and bone resorption by interleukin-4 and interleukin-13 is*

associated with increased osteoprotegerin and decreased RANKL and RANK in a STAT6-dependent pathway. J Biol Chem, 2006. **281**(5): p. 2414-29.

131. Sato, T., et al., *Donepezil prevents RANK-induced bone loss via inhibition of osteoclast differentiation by downregulating acetylcholinesterase.* Heliyon, 2015. **1**(1): p. e00013.
132. Zhou, Z., et al., *HMGB1 regulates RANKL-induced osteoclastogenesis in a manner dependent on RAGE.* J Bone Miner Res, 2008. **23**(7): p. 1084-96.
133. Park-Min, K.H., et al., *Negative regulation of osteoclast precursor differentiation by CD11b and beta2 integrin-B-cell lymphoma 6 signaling.* J Bone Miner Res, 2013. **28**(1): p. 135-49.

APPENDIX

VITA

Hataichanok Charoenpong was born on the August, 9th, 1982 in Bangkok. She received her bachelor's degree, Doctor of Dental Surgery (DDS), from Faculty of Dentistry, Chulalongkorn University in 2004 and worked for 2 following years at Sirindhorn College of Public Health, Chonburi.

Hataichanok Charoenpong completed Master of Science (MSc) and higher graduate diploma program in orthodontics from Chulalongkorn University in year 2008 and 2009 respectively. In year 2012, she graduated MSc in Biomedicine from Lancaster University, United Kingdom and received Thai board of orthodontics in 2015.

Hataichanok Charoenpong worked at Faculty of Dental Medicine, Rangsit University from 2009 until present.